STRAIN RESPONSE IN OSTEOCYTE LACUNA DUE TO MECHANICAL LOADING - A PARAMETRIC FINITE ELEMENT STUDY USING *FEBIO*

A THESIS IN
Electrical Engineering

Presented to the Faculty of the University
of Missouri-Kansas City in partial fulfillment of
the requirements for the degree

MASTER OF SCIENCE

by
SRAVAN KUMAR REDDY KOLA
B. TECH., Jawaharlal Nehru Technological University, 2013

Kansas City, Missouri
2016

STRAIN RESPONSE IN OSTEOCYTE LACUNA DUE TO MECHANICAL LOADING - A PARAMETRIC FINITE ELEMENT STUDY USING *FEBIO*

Sravan Kumar Reddy Kola, Candidate for the Master of Science Degree

University of Missouri-Kansas City, 2016

ABSTRACT

Osteocytes are the major type of living cells in bone and are known to be responsible for the biomechanosensory functions within the bone matrix. Osteocytes are activated by mechanical forces and regulates both osteoclasts and osteoblasts for bone resorption/formation. Not all the osteocytes are activated due to the applied mechanical loading because of many factors such as variation in size, position and orientation of them with respect to the loading surface. Strain response of osteocyte to the applied loading is of importance in estimating the bone resorption/formation. Although previously there were many studies that investigated strain responses at the osteocyte lacuna, very few were finite element studies and were limited to 2-dimensional models. Here in this study, a finite element model was created using *FEBio* at the microscale level and osteocyte lacunar and perilacunar responses were calculated based on three studies: 1) variation in lacunar position, 2) variation in lacunar orientation and 3) variation in lacunar size. A parametric study was performed by varying the elastic modulus of the perilacunar matrix which resulted in a decrease of maximum strain in lacuna with an increase in perilacunar modulus from 5GPa to 20GPa. Then, the model was scaled down to nanometer range and the lacunar responses were investigated and the results were compared with a previous study. Finally, a 3-dimensional osteocyte model was developed using MIMICS and 3-Matic softwares using confocal image stack of mouse femurs.

APPROVAL PAGE

The faculty listed below, appointed by the Dean of the School of Computing and Engineering have examined a thesis titled 'Strain Response in Osteocyte Lacuna due to Mechanical Loading - A Parametric Finite Element Study using *FEBio*' presented by Sravan Kumar Reddy Kola, candidate for the Master of Science degree, and certify that in their opinion it is worthy of acceptance.

Supervisory Committee

Ganesh Thiagarajan, Ph. D., P.E., Committee Chair

Department of Civil and Mechanical Engineering

Mark L. Johnson, Ph.D.,

Department of Oral Biology and Craniofacial Sciences

Cory Beard Ph.D.,

School of Computing and Engineering

TABLE OF CONTENTS

LIST OF ILLUSTRATIONS

Figure Page

LIST OF TABLES

Table Page

ACKNOWLEDGEMENTS

Primarily, I am thankful to the God for the blooming health and well-being that were required to complete this research. Many individuals supported me to make this thesis a reality. I would like to express my deepest gratitude to all of them.

I would like to convey my sincere gratitude to my advisor Dr. Ganesh Thiagarajan for the continuous support of my thesis related research, for his patience, motivation, and immense knowledge. I am highly indebted to him for his constant supervision and guidance. I am thankful to you for making me a part of this research and also for funding this work. I extend my thanks to my thesis committee- Dr. Mark Johnson and Dr. Cory Beard- for their valuable time in reviewing my work.

I am so thankful to Dr. Mark Begonia for the stimulating discussions we had on the ongoing research work which led me all the way in interpreting the results. And I want to extend my sincere thanks to all of my friends and lab mates who stood behind me throughout my journey at UMKC.

Finally, I must express my very profound gratitude to my parents Mr. Kola Samba Siva Reddy and Mrs. Kola Bhulakshmi, to my brother Kola Jagannadha Reddy and my sister Dr. Kola Viraja for providing me with unfailing support and continuous encouragement throughout my years of study and through the process of researching and writing this thesis. This accomplishment would not have been possible without them.

I would like to acknowledge one and all, who directly or indirectly, have lent their hand in this research work.

CHAPTER 1

INTRODUCTION

Bone is one of the denser tissues in human body which though is rigid but is a living tissue and is active in metabolic activities. Bone tissue comprises of three living cells namely osteocytes, osteoclasts and osteoblasts of which osteocytes comprise 95% of the bone cells. In an adult skeleton there is an average estimate of around 42 billion osteocytes whereas the dendritic processes from these cells is approximated to 3.7 trillion [1](Pascal R. Buenzli, *et, al.,* 2015). From research studies, it is evident that all the living organisms from bacteria to human beings are mechanosensitive to the stimulus. Such mechanosensitive systems are present in the human body at each cell in one or the other form [2](A. Wayne Orr, *et, al.,* 2006). According to the Wolff's theory, which was proposed in the nineteenth century, bones adapt their structure and mass to the mechanical stimuli to increase the load handling capacity [3](A. Santos, *et, al.,* 2009). Mechanotransduction is a process in which the physical/ mechanical forces are transformed into biological responses. Osteocytes are considered to be the mechanosensory cells in the human bone and are responsible for orchestrating bone modeling/ bone resorption/formation through the activity of osteoclasts and osteoblasts [4](Chenyu Huang, *et, al.,* 2010). The process of mechanotransduction in bone is shown in figure 1-1 which shows the process by which the mechanical forces applied on the bone matrix deforms it. As the osteocytes occupy a fluid filled network that have lacunae interconnected through thin channels called canaliculi, the deformation caused by mechanical loading stimulates the osteocytes. Then osteocytes signal osteoclasts/ osteoblasts through the canalicular network for bone remodeling.

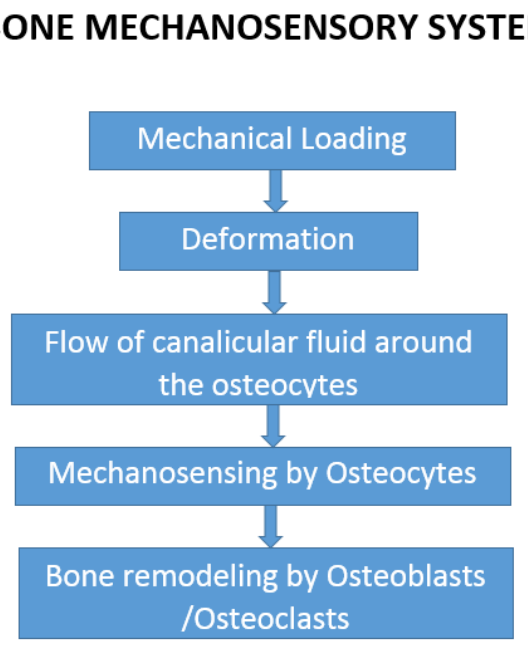

Figure 1-1: Process of Mechanotransduction in bone

The results from series of experiments [5](Forwood, *et al.*, 1996) concluded that dynamic loading has an effect on bone remodeling whereas static loads had no such effect. One of the consequences of bone remodeling activity is mechanically adaptive control of bone architecture that depends on the relationship between loading imposed and the prevailing bone architecture. This relationship is dependent on the strains in the bone matrix and these strains can be used as controlling variable for the adaptive process [6](L. E. Lanyon, 1993). The mechanical loads are more effective in intensifying the bone formation if short period discrete loads are applied with recovery periods rather than continuous application of the loads [7](A. G. Robling, *et al.*, 2002). The experiments conducted on rat tibia [8](D. B. Burr, *et al.*, May 2002) suggest that a recovery period of 4-8 hours is ample time for a bone to reestablish its mechanically sensitive state. In bone matrix, structural components such as canaliculi, osteocyte lacunae and perilacunar regions are considered to be potential stress concentrators

and local microstructural strains at these locations are different from the macrostructural strains [9](Nicolella, *et al.,* 2005). Finite element models are best suitable for estimating strain responses at the microstructural level.

A parametric study was conducted using a finite element model was developed by [10]Bonvitch, *et al*., 2006, to study the tissue strain amplification at the osteocyte lacuna. The results from that model on tissue strain amplification at osteocyte lacuna showed that as the perilacunar modulus decreases the perilacunar tissue strain increases. Higher strains were observed for the perilacunar region with a modulus of 15GPa compared to the perilacunar region with a modulus of 35GPa. Based on this study we have processed further by making similar approximations and extending our work with different studies.

The software programs we have used in implementing this model are discussed as a part of chapter 2. In this chapter, a step by step procedure of creating the model, executing the model and also analyzing the results are discussed. Apart from these explanations, other software tools that are supported by the software are described.

In this thesis work, the third chapter deals with the materials I have used in the design of the model and the models created in a chronological order for this study are explained in detail. The material properties assigned to different structures within the bone matrix are shown. In addition to these details, boundary and loading conditions which are considered as an important factor for the process of mechanotransduction are also explained in relation to each model.

The fourth chapter in this work focusses on the parameters that are responsible for the strain magnification in the bone lacuna or perilacuna. This chapter includes a detailed explanation of selection of the lacunae considered in the calculation of strain responses in

every model. Also, a parametric study is done for every model by varying the elastic modulus value in the perilacunar tissue.

The work in fifth chapter especially focusses on the results obtained from various simulations of *FEBio* and the observations I had during the analysis. In this chapter, the results are grouped based on the classification done in the previous chapters. Then the results from one study are compared with others to see whether all the models were responding in the same fashion.

The sixth chapter presents the conclusions of this thesis work and the future scope of work. In this chapter, I have included the details of how this work can progress to the next level. In the final chapter, the analysis procedure I had followed during my entire thesis work has been clearly explained.

CHAPTER 2

SOFTWARE DESCRIPTION

2.1 Overview of *FEBio*:

FEBio is a software suite developed by [11]Maas *et al*., 2012 in musculoskeletal research laboratories at the University of Utah. *FEBio* is the acronym for Finite Elements for Biomechanics. It is a non-linear finite element solver designed especially for applications in biomechanics. Tissues in the human body can interact in many different and complicated ways. *FEBio* is the software package that supports a wide range of material models to model various types of tissue. Different loading and boundary conditions can also be modeled. These include but not limited to fixed or prescribed displacements, mechanical forces such as nodal and pressure forces. The official website *www.FEBio.org* includes all the required software tools to setup this finite element solver environment. *Preview* is the preprocessing software package designed to generate input files for *FEBio*. In *Preview*, finite element models are created based on the dimensions, material properties and meshing requirements of the problem and are subjected to certain loading and boundary conditions. *Preview* is also capable of importing models that are created in other softwares like LSDYNA, ABAQUS, Hyper Mesh, NIKE 3D and more. *Preview* models are processed using *FEBio*. *Postview* has been designed with several post processing capabilities like creation of surface plots, plane cuts, etc. and is used to view the *FEBio* output files. *Postview* also offers a very user friendly interface that has features for creating the 3D view for the existing finite element models. It also supports LSDYNA keyword and database files, NIKE3D input and output files in addition to *FEBio* output files. In short, the finite element models are created using *Preview* which are processed in *FEBio* and finally viewed in *Postview* for analysis.

2.2 Creating a sample model:

The finite element models analyzed in this thesis work were created using three interrelated softwares namely *Preview*, *FEBio* and *Postview* that were already introduced in the previous sections. In this section, we explain each and every detail of modeling in a step by step procedure. We start our modeling by using the preprocessing tool, *Preview*, for creating our model.

Step #1: Open *Preview* modeling interface

Whenever we install the *Preview* software, a desktop icon is automatically created. The *Preview*.exe file can be opened by double-clicking on that icon.

Step#2: Selection of geometry

Depending on the model requirements, we can select the geometry of the object (say bone in our case) from different choices (like rectangular, cylindrical, spherical, etc.) available. All these choices can be found under the create context tab. After selecting the geometry, we need to specify the dimensions of our geometry like width, height and depth. Then, click on create. We can see the geometry appeared in the modeling interface after clicking the create button. One can have the choice of selecting the position of geometry to be placed in the modeling space by just assigning required numbers to the x, y and z dimensions. All these options can be seen in figure 2-1.

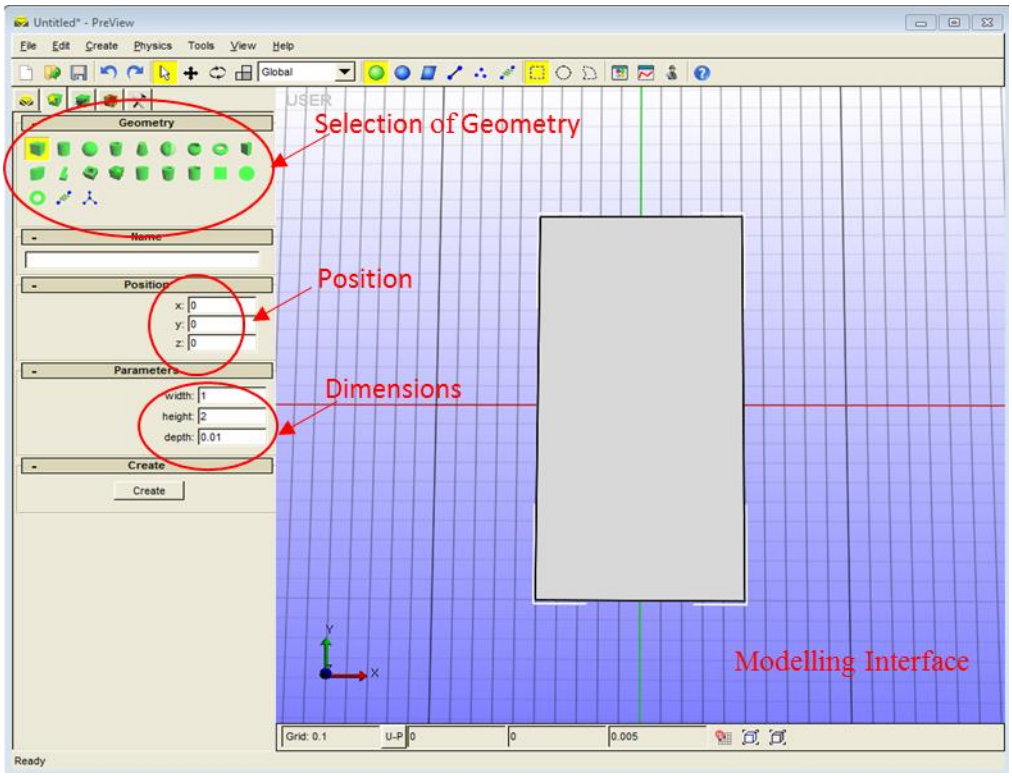

Figure 2-1: Selection of geometry in *Preview* modeling

Step#3: Creating mesh

Select mesh tab, where we can specify meshing requirements for our model. We can choose different types of meshing methods like hexahedral or tetrahedral. Here, we need to specify the number into which the mesh has to be divided for each coordinate axis according to our requirement. In order to see the mesh lines on the model, select *View/ Toggle Mesh lines* or press ‘m’. Meshing is the technique through which one can analyze the model at its elemental level. The application of mesh parameters is shown in figure 2-2.

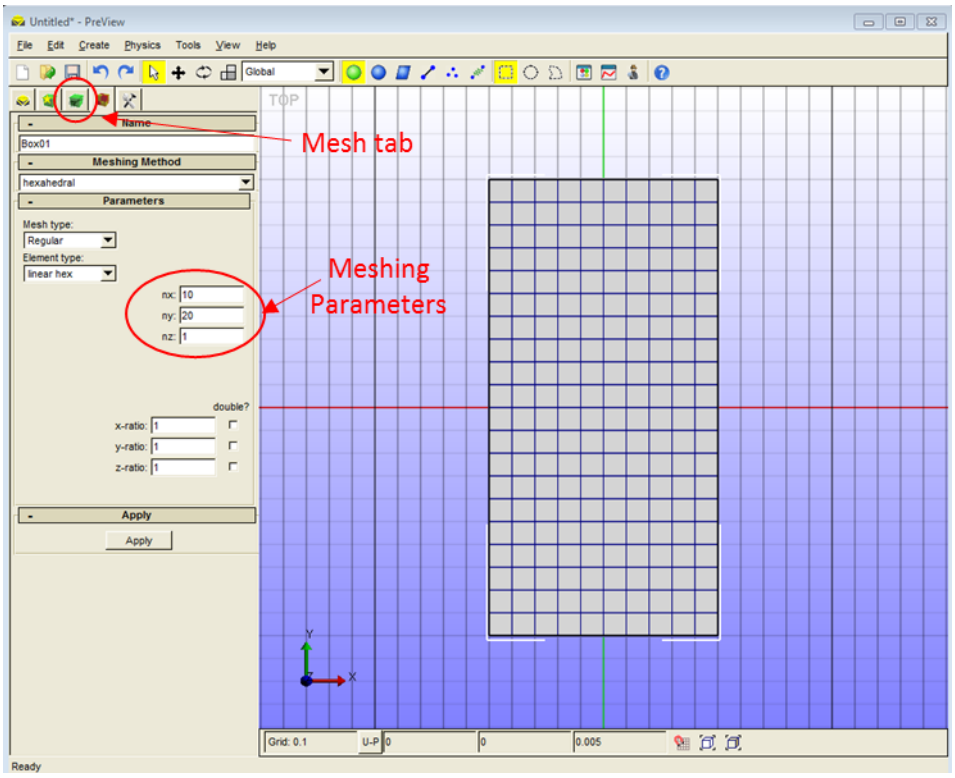

Figure 2-2: Application of mesh parameters to the model

Step #4: Creating Partitions

Our model is comprised of three types of elements namely bone, lacuna and perilacuna. For each type of element, we need a separate partition so as to assign material properties to them. In order to do that, we need to convert the mesh to editable one by using the *editable mesh* drop down as shown in figure 2-3. In this window, we can also modify the dimensions of our model created in step #2.

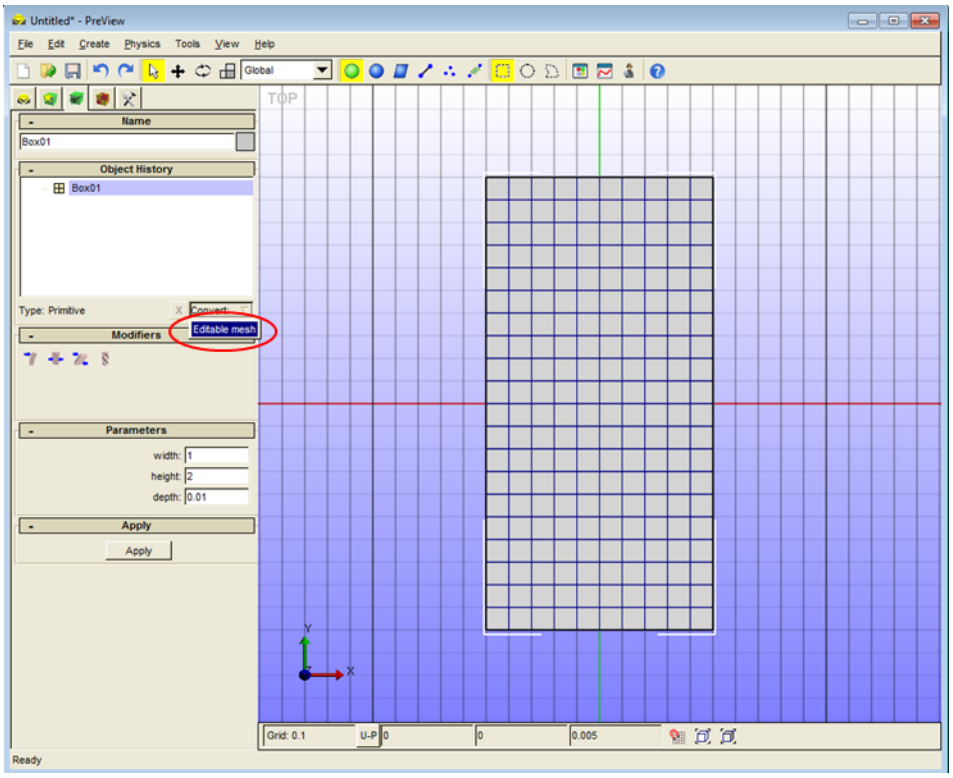

Figure 2-3: Conversion of mesh to an editable mesh

After converting the mesh to an editable one, we have a choice of selecting elements, faces or nodes in the mesh tab. In our case, we select elements and make them into a separate partition as shown in figure 2-4. Here we have a choice of assigning elements to a particular partition also by using the partition numbers. This way we have created separate partitions for bone, lacuna and perilacuna.

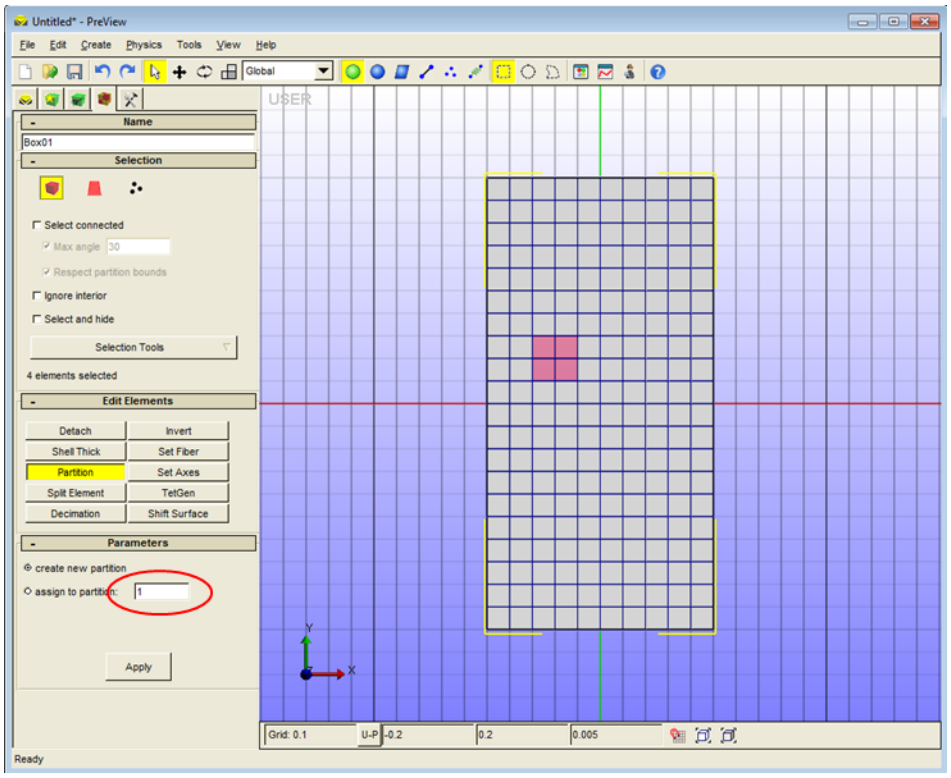

Figure 2-4: Selection of elements and creating partitions

Step #5: Assigning material properties

As we are having three different types of materials, in order to differentiate them we need to assign different material properties based on their original characteristics. In this step, we are going to represent a particular material by assigning its properties in the finite element model. Although it is known that bone is anisotropic in nature, as a starting point we have represented the bone material to be isotropic elastic in finite element models. The properties to be defined in the material includes density, elastic modulus and the Poisson's ratio. These property values are assigned in their respective fields. The partition related to the material is selected and is assigned to the material as shown in figure 2-5. Similarly, the other materials are also defined.

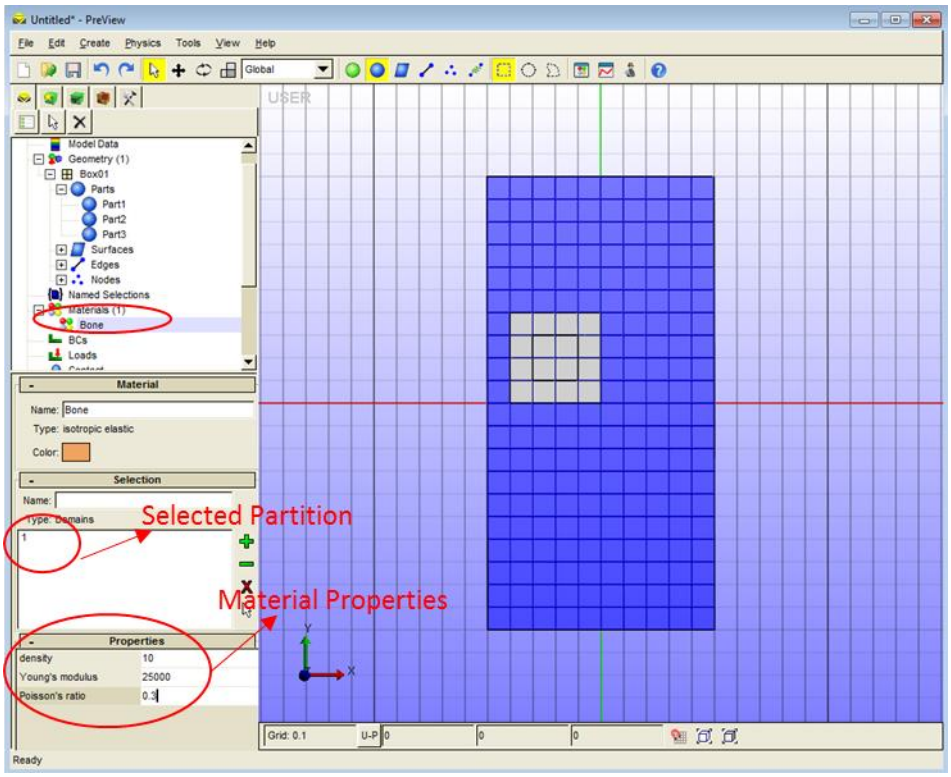

Figure 2-5: Assignment of material properties

Step #6: Applying loading and boundary conditions

In this step, we are applying boundary conditions as well as boundary loads. In our model, the bottom surface is fixed in all the three dimensions while a pressure load is applied on the top surface. This can be done by adding the boundary condition (BC) or boundary load (load) and assigning the face to it on which we want to apply BC or load. This procedure is shown in figure 2-6.

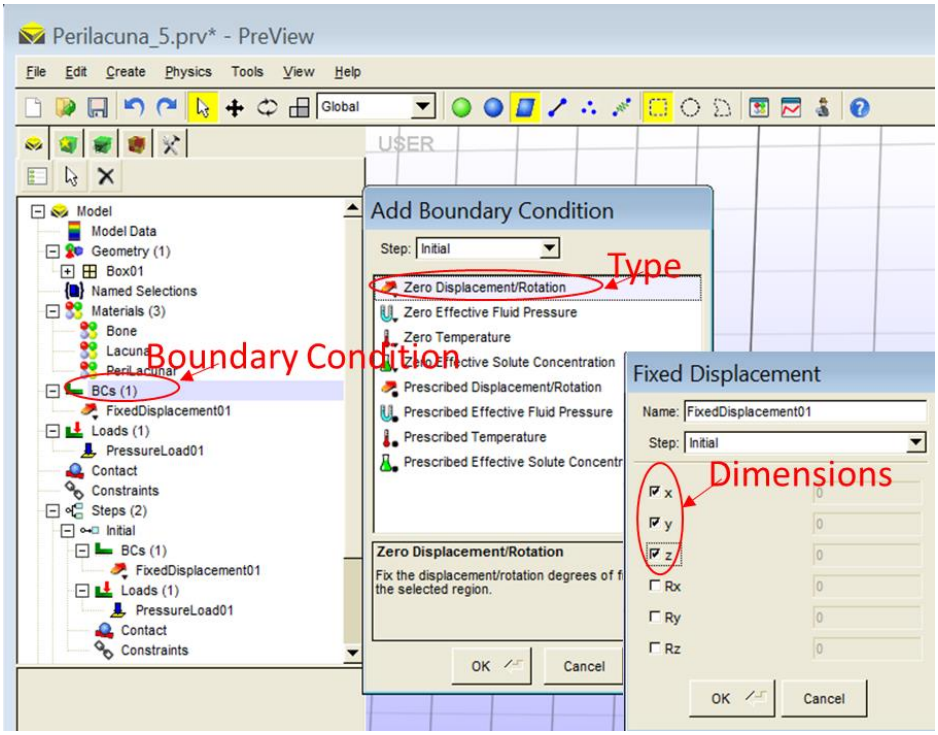

Figure 2-6: Applying boundary conditions to the model

Boundary loads are of different types depending on our requirement. In our model, we have applied a pressure load. After selecting the pressure load as shown in figure 2-7, load factor should be assigned and it is determined by global bone strains which will be discussed in the later sections.

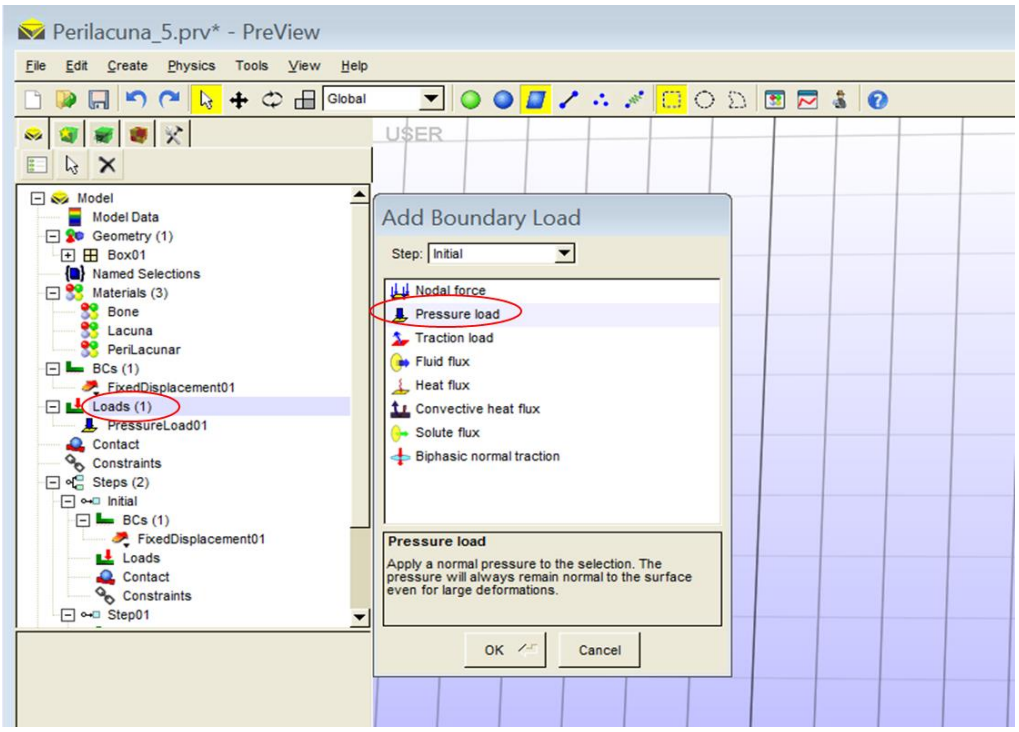

Figure 2-7: Applying load to the model

Step #7: Save and export

Now save the file as .prv and then export it to *FEBio* as a .feb file.

2.3 Executing the model:

The model created in the *Preview* interface was exported and saved as *FEBio* file. Thus, the model can be executed in the *FEBio* software tool in many methods of which the ones used during this work are described here.

(i) The *FEBio* Prompt

The *FEBio* prompt is one of the faster and easier methods to execute the .feb file. In this method, we need to first start *FEBio* program. The *FEBio* prompt will open and it looks like a command window. We should the file here by using the 'run' command. The commands used in the *FEBio* prompt are given below

help: to view all of the available commands and a description for each

quit: to exit *FEBio*

run: to run a .feb input file

version: to print the software version details

Figure 2-8 shows the *FEBio* prompt and the command used for the execution of the *FEBio* file that was in a particular file location (e.g. C:\Users\skfc3\Desktop\Perilacuna_5.feb).

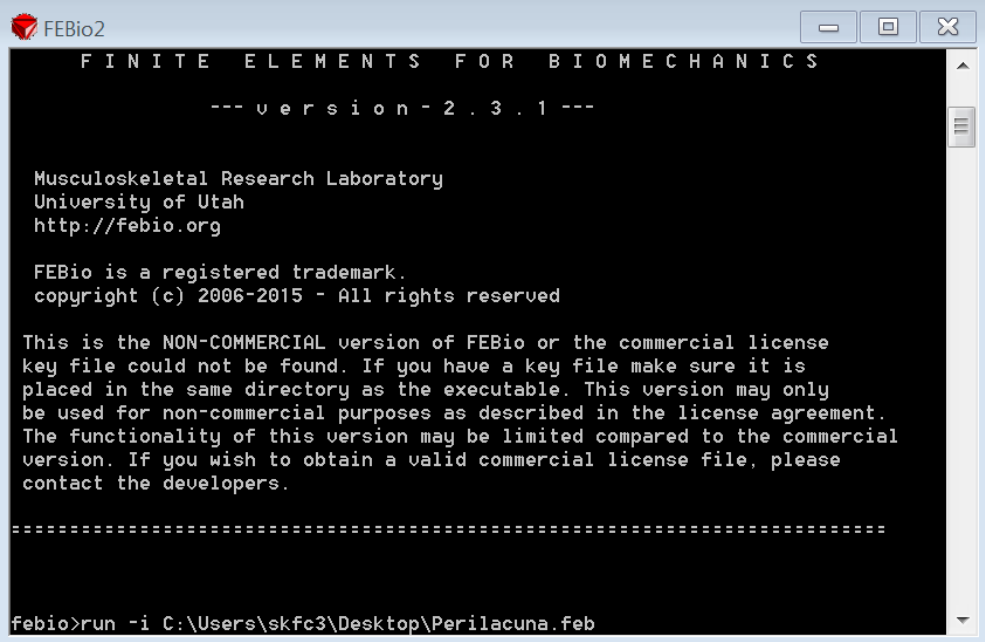

Figure 2-8: Execution of the model in *FEBio* prompt

(ii) File Explorer

This method is very convenient and easy to run *FEBio* input files. In this method, we first navigate to the folder that contains our *FEBio* input files through File Explorer. Now, right-click on the *FEBio* input file and select *Open with* from the drag down menu. Then select *Choose default program* as shown in figure 2-9. A list of programs is displayed and we can select *FEBio* from that list. If we can't find *FEBio* on this list, then click the *Browse* button at the bottom and navigate to the executable file location (e.g. in C:/Program Files/*FEBio*-

2.4.2/bin), select it and click on the *Open* button. Then select *FEBio* in the *Open With* drop down menu and click Ok.

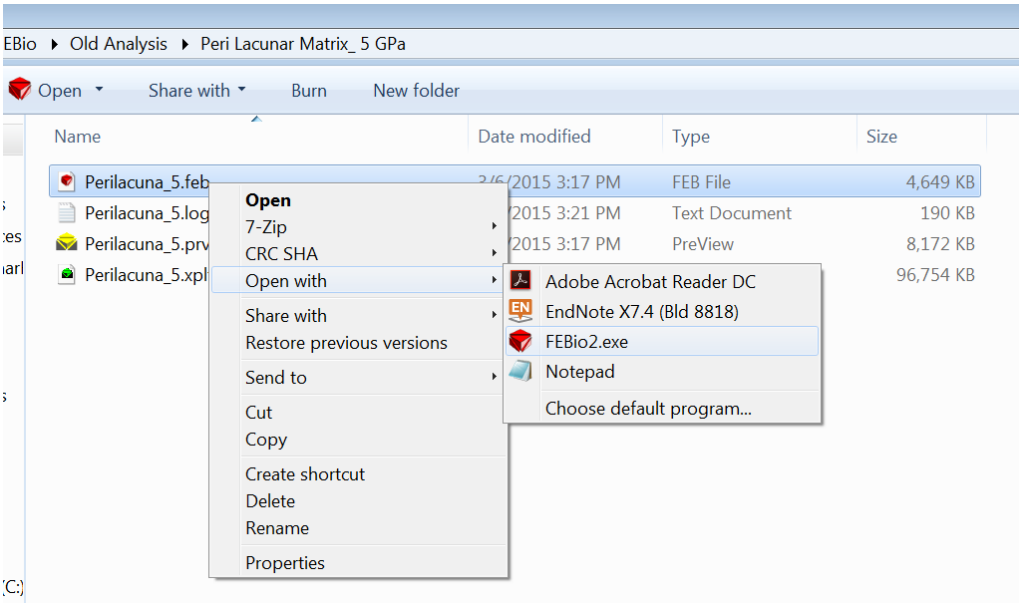

Figure 2-9: Opening a file in Windows explorer

After this, the execution process is simple. Just double click on the *FEBio* input file and the execution starts as shown in figure 2-10.

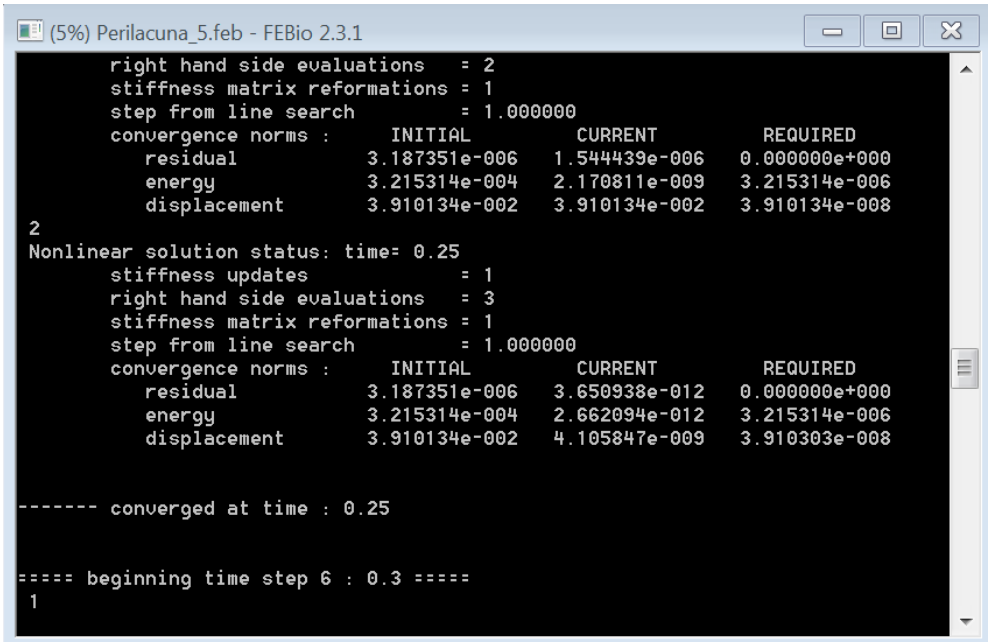

Figure 2-10: Execution of *FEBio* file using file explorer method

After the execution is done, we find a log file (.txt) and a *Postview* file (.xplt) sharing the same folder in which .prv and .feb files are present as shown in figure 2-11.

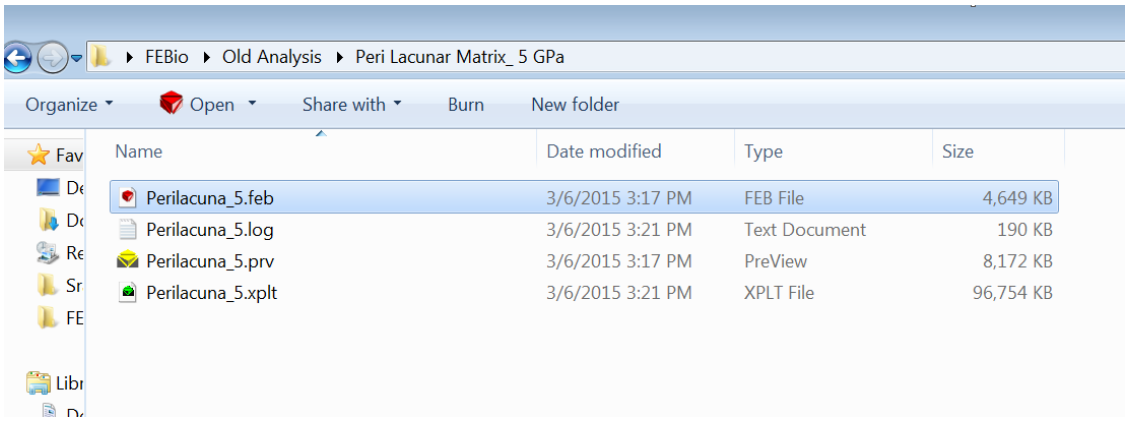

Figure 2-11: Creation of Log file and *Postview* file

2.4 Analyzing the model:

Postview files will be automatically created upon the execution of the *FEBio* (.feb) files and these files were used in the analysis of our models. A file with an xplt extension is the *Postview* input file. To open this type of file, we need to just navigate to the file and double click on it. Upon opening the *Postview* file, we are able to view and have accessibility to perform operations on the model in the *Postview* graphical interface as shown in figure 2-12.

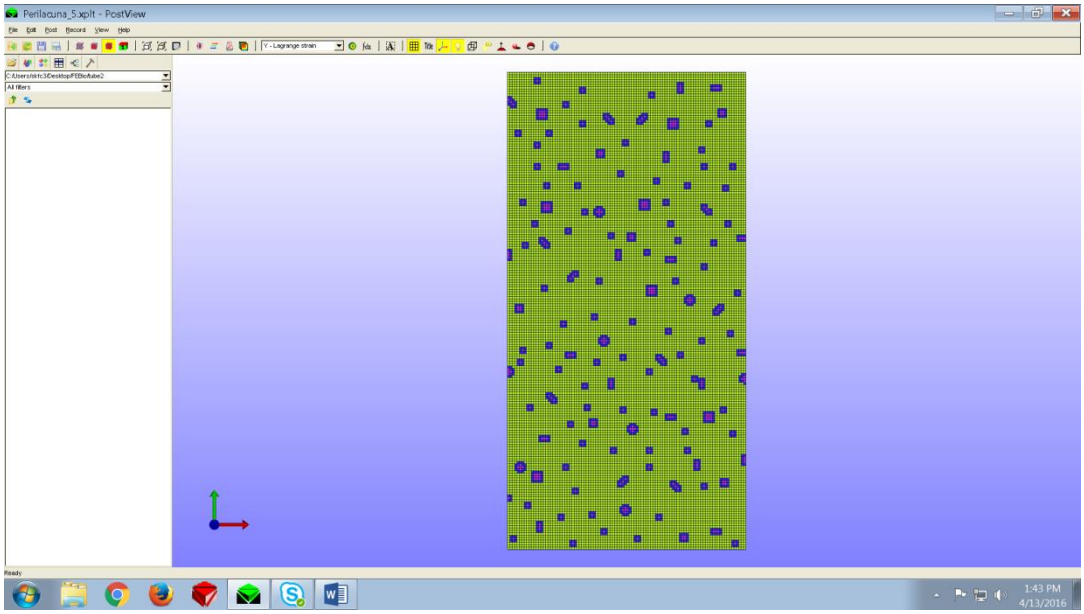

Figure 2-12: *Postview* user interface

In this graphical interface, each model can be analyzed at the elemental level and the instantaneous values of variables such as displacement, stress and strain can be obtained at different time instants.

CHAPTER 3

MATERIALS AND METHODS

3.1 Materials:

Bone is anisotropic or orthotropic in nature which means that its elastic properties are different in all directions. The stress and strain magnitudes within a bone matrix are not only dependent on the applied mechanical load, but are also influenced by material properties such as density, Young's modulus and Poisson's ratio of the bone, osteocyte lacuna and perilacuna. The finite element modeler is responsible for selecting different material properties for each type of structure. The Young's modulus which is also known as elastic modulus (E) is defined as the ratio between the uniaxial stress and strain (σ/ϵ) and it is measured in compression or tension. It defines the stiffness of the material. Poisson's ratio (ν) is defined as the negative of the ratio of the lateral strain to axial strain.

There are many approaches to extract material properties that were used in the model and of which literature survey is simple and advantageous. Based on the previous work by [12]Bonivtch, et al., 2006, in this study bone tissue was modeled as an isotropic elastic material with three material regions namely bone, lacuna and perilacuna. An elastic modulus value of 25GPa was selected for bone tissue, 0.1 MPa was selected for lacunar tissue and a range of 5GPa to 20GPa was selected for perilacunar tissue. A Poisson's ratio value of 0.3 was used for both bone and perilacunar matrix whereas a value of 0.1 was used for lacuna. All the material properties are shown in table 3-1.

Table 3-1: Material properties of the finite element model

Property	Bone	Lacuna	PeriLacuna
Type	Isotropic Elastic		
Density (mass per mm^3)	10	1	10
Young's Modulus (GPa)	25	0.1	5 - 20
Poisson's ratio	0.3	0.1	0.3

3.2 Micro Model:

In this section, the preliminary bone model which was designed for our study was shown with details of meshing, nodes and different shapes and sizes of lacuna used. A simple rectangular geometry was created, representing bone, in the *Preview* modeling interface and the size of bone matrix was taken as 1 mm x 2 mm x 0.01 mm. Meshing was performed to this model using hexahedral meshing method and the meshing parameters were chosen in such a way that each element size was brought down to 10 µm x 10 µm x 10 µm. This model consists of 40,602 nodes and 20,000 elements in total. The dimensions of the model and individual element are shown in table 3-2.

Table 3-2: Dimensions of the Micro model

Dimension	Entire Model	Single Element
Width	1 mm	10 µm
Height	2 mm	10 µm
Depth	0.01 mm	10 µm

Figure 3-1 represents the bone model with dimensions shown in table 3-2. This bone matrix was divided into three partitions: 1) Bone, 2) Lacuna and 3) Perilacuna. The material properties to these partitions were assigned based on literature survey details and were discussed earlier in materials section.

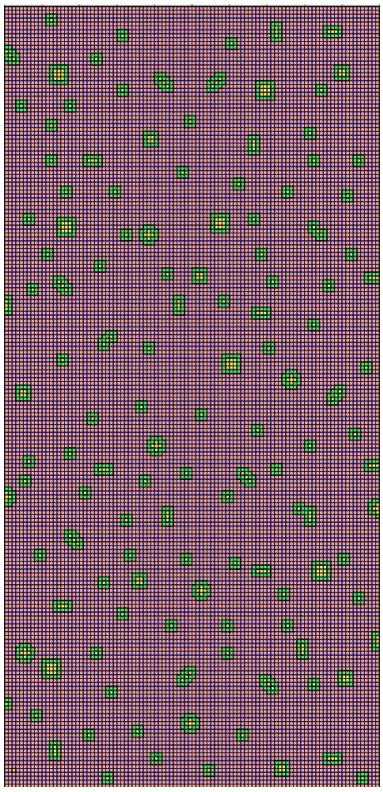

Figure 3-1: Micro Model - *Preview*

A zoomed in portion of the above model is as shown in figure 3-2 in which osteocyte lacunae were modeled in different shapes with lacunar elements in the center of each structure surrounded by a layer of perilacunar elements on all sides. All the non-structured elements were bone matrix elements.

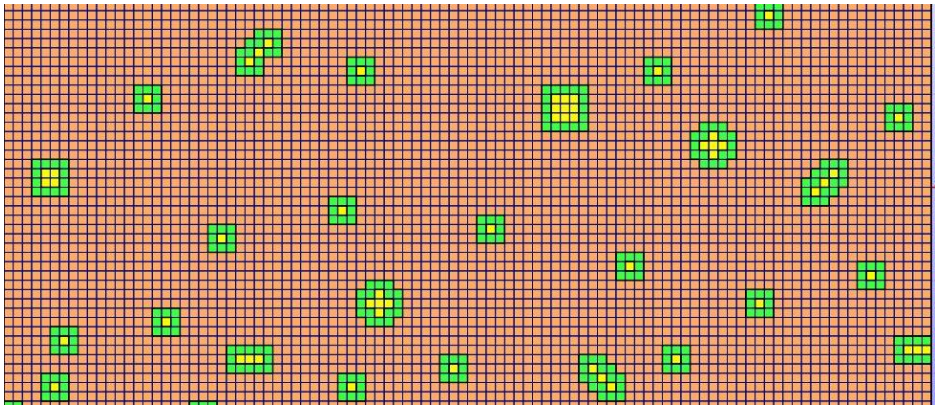

Figure 3-2: Zoomed view of a small portion of the Micro model

There was no specific pattern followed to create lacunar structures in this model. The lacunae were assigned different sizes and shapes in this model for the parametric study that was performed by using the position, orientation and size variations of the lacuna.

3.3 Nano Model:

The size of the bone matrix considered in the previous model was of micrometer range in all the dimensions. Also size of each osteocyte considered in that model doesn't match up with the actual size of an osteocyte. In order to resolve the actual size of the osteocyte in a detailed manner, a nanoscale model was developed based on the size of the osteocyte of approximately 20 µm x 8 µm x 4 µm [13](Rochefort, *et al*., 2010). Each osteocyte was modeled as an oval shape in order to resemble an actual osteocyte.

A rectangular solid bone geometry of 0.08 mm x 0.16 mm x 0.004 mm was created. In this model, the hexahedral meshing method was used and meshing parameters were selected in a way to make each element size as 0.8µmx0.8µmx4µm. This nanomodel was comprised of 40,602 nodes and 20,000 elements. The dimensions used in creating the nanomodel are shown in table 3-3.

Dimension	Entire Model	Single Element
Width	0.08 mm	0.8 μm
Height	0.16 mm	0.8 μm
Depth	0.004 mm	4 μm

Table 3-3: Dimensions of the Nano model

Figure 3-3 represents the nano model that was created with the dimensions specified in table 3-3. Similar to the micro model, bone matrix was divided into same three partitions: 1) Bone, 2) Lacuna and 3) Perilacuna. Material properties were also the same as the micro model and were shown in table 3-1. Here in this model, all the osteocytes have 122 lacunar elements and 106 perilacunar elements.

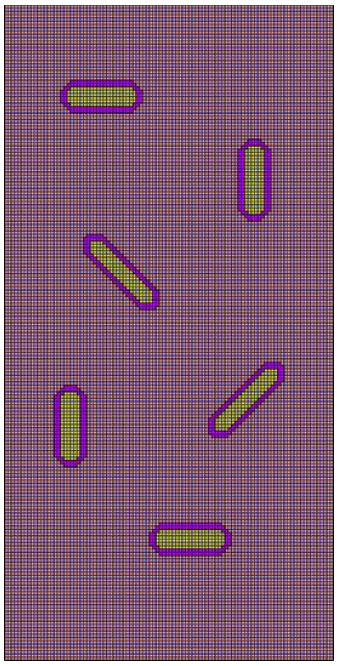

Figure 3-3: Nano Model – *Preview* representation

In this model, six osteocytes were modeled (as shown in figure 3-3) in different positions and orientations to examine their strain response to axial loading. Figure 3-4 further shows the details of a single osteocyte/lacuna with bone elements, lacunar fluid space, cell body and perilacuna as labelled in figure 3-4. Parametric studies were conducted on the nano model similar to the one conducted for the micro model.

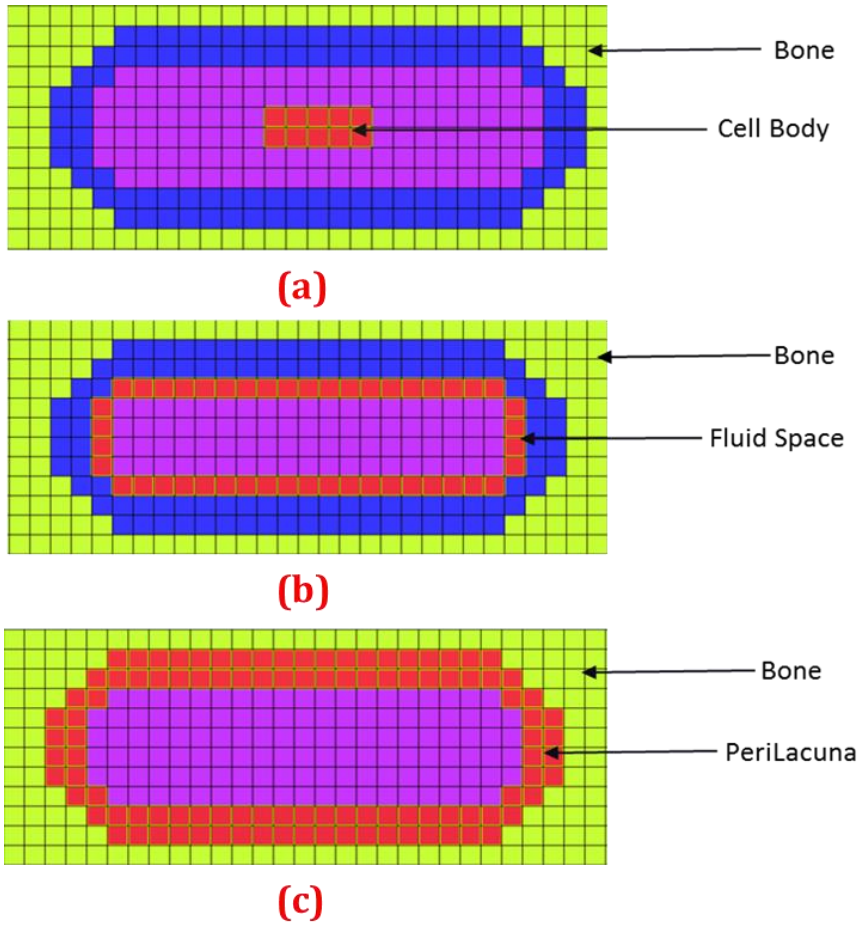

Figure 3-4: Partitions in the Nano model – Bone, Lacunar fluid space, Cell body and PeriLacuna

3.4 Osteocyte 3D Model:

In both of our previous models, the micro model and the nanomodel, although we had the third dimension physically, we restricted it to a constant value depending on the dimensional requirements of the osteocyte. In this 3-D model, actual osteocytes from 5-month

old mouse femur was imaged using confocal imaging microscope and used for modeling the Osteocyte 3D model. This work was done in conjunction with Dr. Sarah Dallas and Dr. LeAnn Teide from UMKC school of Dentistry. Dr. Ganesh Thiagarajan, a Professor at UMKC School of Computing and Engineering, created this model by stacking the confocal images together into a bone matrix by using MIMICS innovation software suite and 3-Matic software. Figure 3-5 was taken from the MIMICS software which features the 3 dimensional model with 17 osteocytes inside the bone matrix.

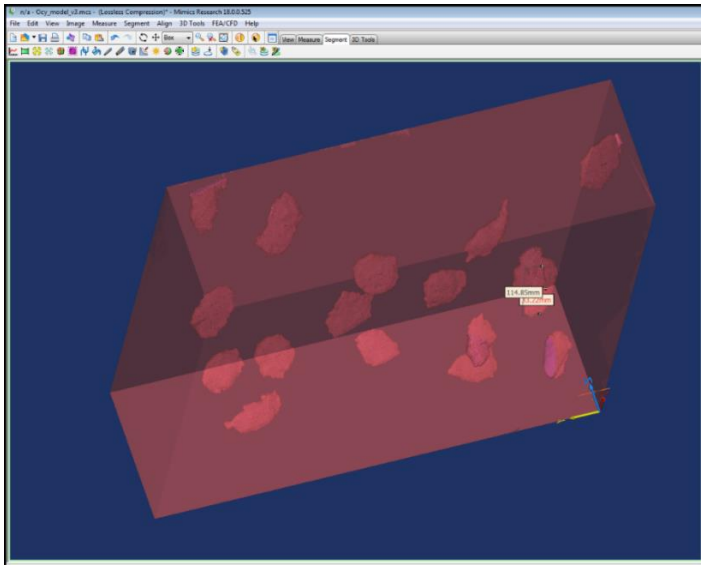

Figure 3-5: Osteocyte 3D Model designed using Mimics software

Using 3-Matic software, osteocytes and bone matrix were divided into separate partitions. Tetrahedral meshing method was used for mesh generation. Then this finite element model created in 3-Matic was exported to *Preview* where loading and boundary conditions were applied to the model. Material properties were assigned to osteocytes and bone as discussed in materials section. Figure 3-6 represents the *Preview* of the Osteocyte 3D model in which blue colored structures are the lacunae and bone matrix is shown in grey color. The osteocyte 3D model comprised of 137,736 nodes and 530,205 elements.

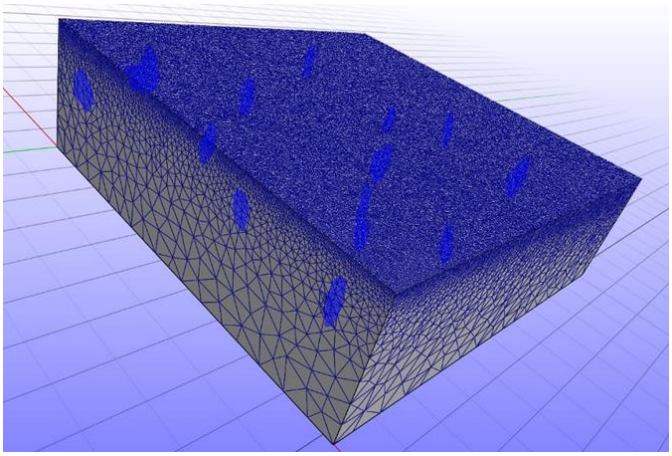

Figure 3-6: *Preview* of Osteocyte 3D model with bone matrix and osteocytes

All the 17 osteocytes were of different sizes and were positioned randomly. Based on their position and size, a study was performed to determine the behavior of the model to the applied pressure load.

3.5 Loading and Boundary Conditions:

This section provides the loading and boundary conditions applied in the 3D model. Lanyon, *et, al.*, 1984 concluded that bone resorption/ remodeling was influenced by cyclic loading. Based on that conclusion, we had designed our model with cyclic loading and certain boundary conditions which were discussed in the following sections.

3.5.1 Micro Model:

In the micro model, a compressive cyclic pressure load was applied to the model. Figure 3-7 represents loading cycle and the points on it represents observation points at which the strain responses were measured.

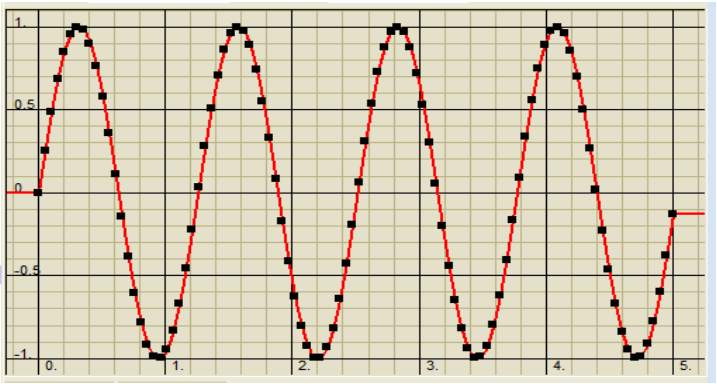

Figure 3-7: Loading cycles with observation points

In the *Preview* modeling interface, an option exists to select boundary conditions and boundary loads. Using these options in our model, pressure was applied as a boundary load on the top surface and the bottom surface was restricted in all the directions by fixing its displacement to zero. Figure 3-8 depicts our micro model with the pressure load applied on the top surface and a zero displacement boundary condition on the bottom surface.

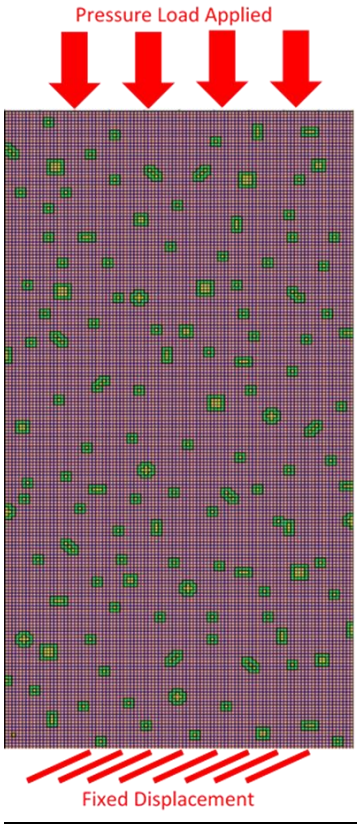

Figure 3-8: *Preview* of Micro model with loading and boundary conditions

3.5.2 Nano Model:

Similar to the micro model, a pressure load of four full cycles was used for loading in the nanomodel with the bottom surface fixed in displacement in all the three dimensions as shown in the figure 3-9. A load factor of 50 was used in this model so as to obtain a global maximum bone strain of 2000 microstrain.

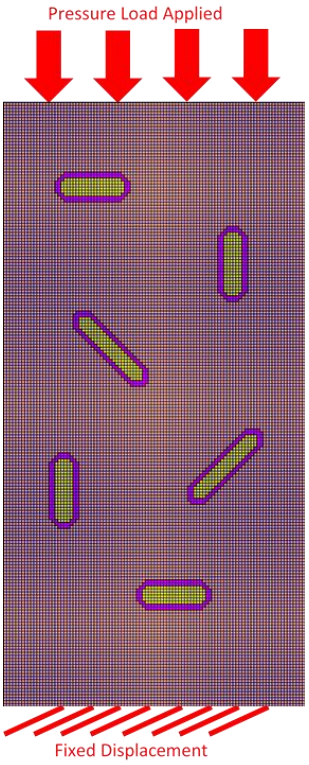

Figure 3-9: *Preview* of Nano model with loading and boundary conditions

In this model, we considered 50 observation points in preprocessing to perform analysis of the model. Figure 3-10 represents the observation points at which strain responses were calculated.

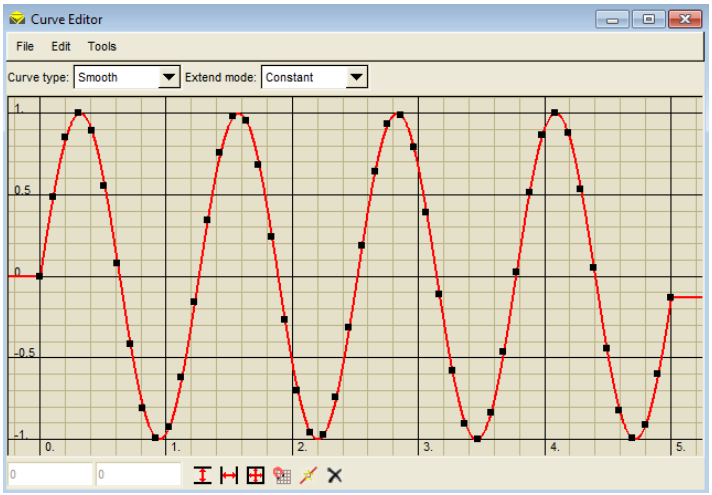

Figure 3-10: Loading cycles with 50 observation points on it

3.5.3 Osteocyte 3D Model:

The osteocyte 3D model was designed with 530,205 elements and 137,736 nodes which were large in number when compared with our previous models. Figure 3-11 demonstrates the loading surface on which the pressure load was being applied and the bottom surface which was not shown in the figure was restricted to a zero displacement in all dimensions.

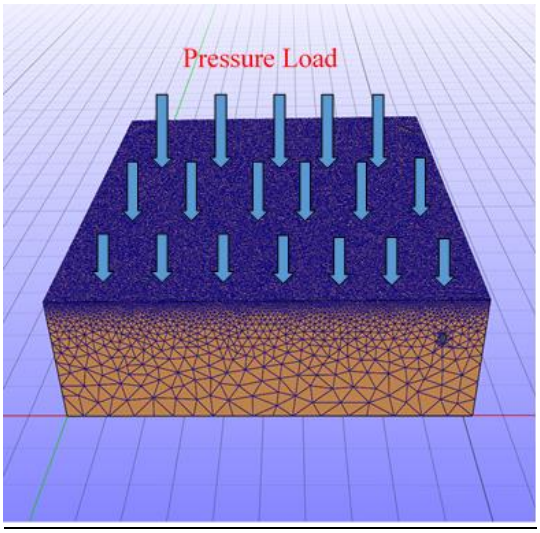

Figure 3-11: *Preview* of Osteocyte 3D model representing loading surface

In the nano model, we observed that the strain responses in the second, third and fourth loading cycles were exact replica of the first loading cycle. Hence, in order to reduce the processing time and memory space allocation, loading was reduced down to less than one full cycle. Figure 3-12 demonstrates the pressure loading cycle with 25 observation points where the analysis was performed in measuring the strain responses.

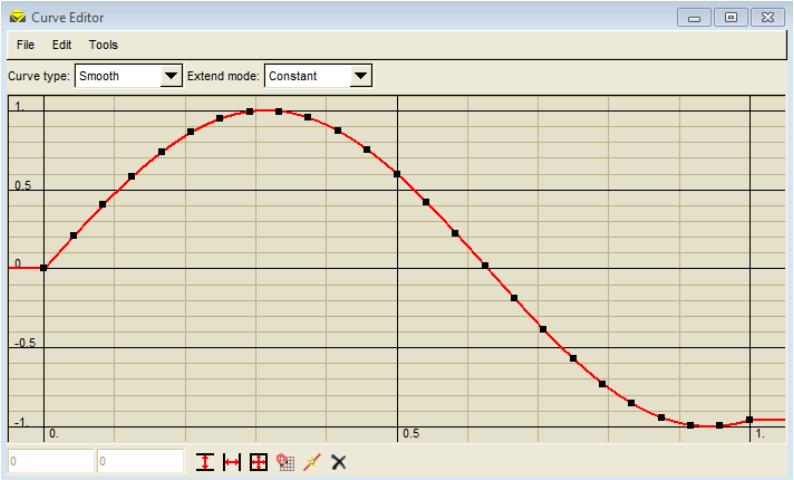

Figure 3-12: Loading cycle and observation points used in Osteocyte 3D model

3.6 Calculation of Bone Strains: (Micro Model)

The previous studies on estimating strain response in osteocyte lacuna by [12]Bonivtch, *et al.*, 2006 proposed a global strain of 2000 microstrain which was considered to be the maximum physiological strain experienced by human bone under active conditions. The magnitude of pressure load applied in our model was approximated to 2000 microstrain by varying the load factor using a trial and error method. For every trial made, average bone strain was calculated from nine elements in the center of the model as shown in the figure 3-13. As the size of the biggest sized lacuna in our model was nine elements, we considered only nine elements in the calculation of bone strain.

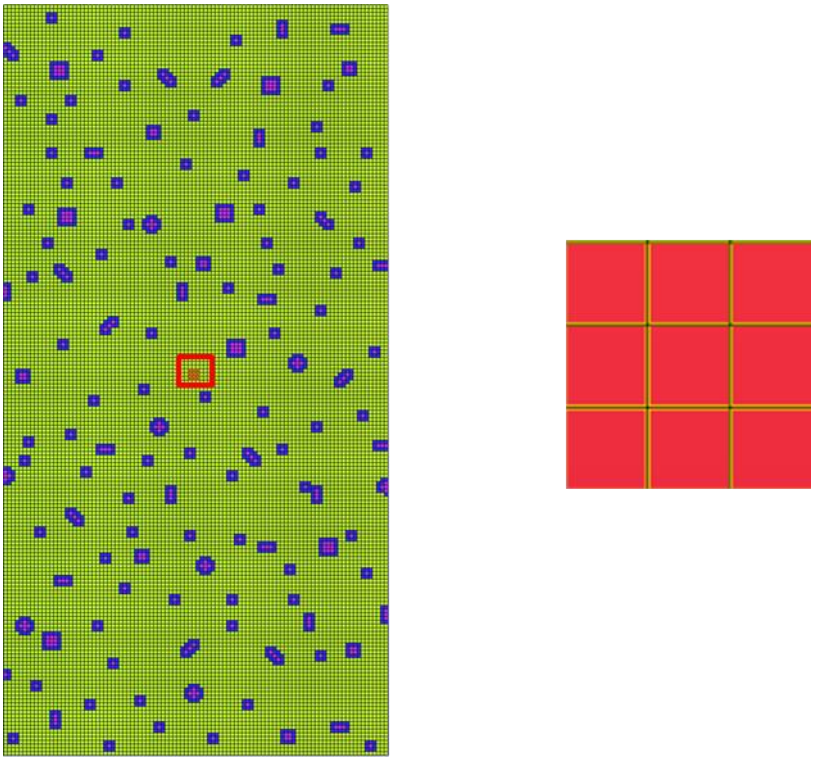

Figure 3-13: Elements considered in the calculation of bone strain

The Y-Lagrangian strain in all the elements at each time instant were taken using Trackview tool in *Postview* as shown in the figure 3-14 and were averaged. The maximum of the averages was taken into account for the bone strain calculations. By trial and error analysis, the maximum strain was approximated to 2000 microstrain.

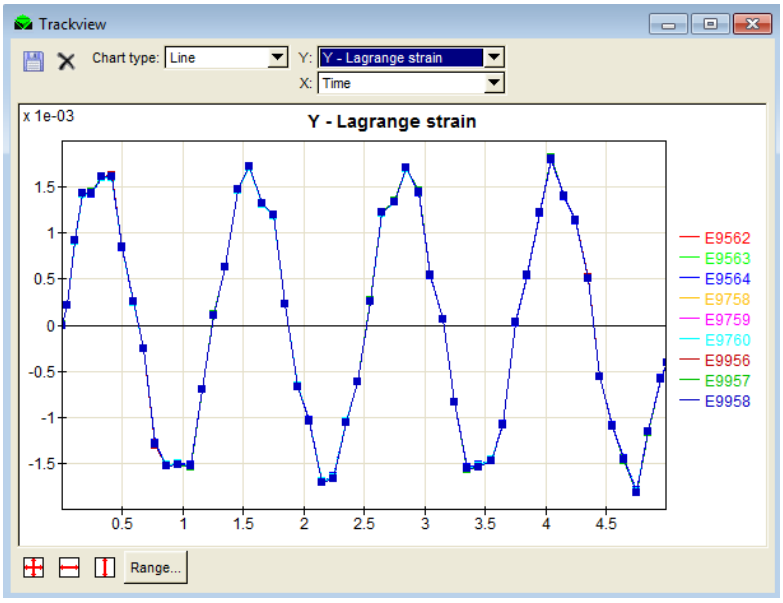

Figure 3-14: Trackview of the elements considered in bone strain calculation

A similar approach was used in the calculation of bone strains for the nano model and the osteocyte 3D model.

CHAPTER 4

PARAMETRIC ANALYSIS

4.1 Introduction

This chapter introduces the parameters that affect the calculations of lagrangian strains in different lacunar and perilacunar elements in our designed models. These include but not limited to position, orientation and size of the osteocyte lacuna. The work on lacunar strain amplification by [12]Bonivtch, *et al.*, 2006 was based on a parametric study by varying the elastic modulus of perilacunar tissue. Hence, in addition to the parameters mentioned above, we had also considered the elastic modulus of the perilacunar tissue and performed the parametric study by varying the elastic modulus in the range of 5GPa to 20GPa.

4.2 Micro Model:

This section introduces the preliminary micromodel parametric analysis. The lacunae in a bone matrix were of the different size and or shape. Hence, in this analysis, we had classified our work in to three different studies in order to evaluate the variation in strain responses with respect to three different parameters. The parameters that were considered in these studies were (i) position, (ii) orientation and (iii) size of the osteocyte lacuna. While studying each parameter separately in each study, we also investigated the effect of the perilacunar elastic modulus on the strain response.

4.2.1 Variation based on Position:

The positional variation in the lacunae is one of the major factor that contributes to the magnification in the strain values. Hence, to determine the magnification in lagrangian strain values, we selected four lacunae, of same size and orientation, at four different positions on

the bone matrix. Each lacuna comprised of 3x3 elements which results in the size of each lacuna to 30 µm x 30 µm. The load was being applied on the top surface while maintaining the bottom surface fixed in displacement in all the three dimensions. Figure 4-1 shows the *Preview* and *Postview* of the micromodel with the four lacunae named, L1 through L4, sequentially with respect to their distance from the loading surface.

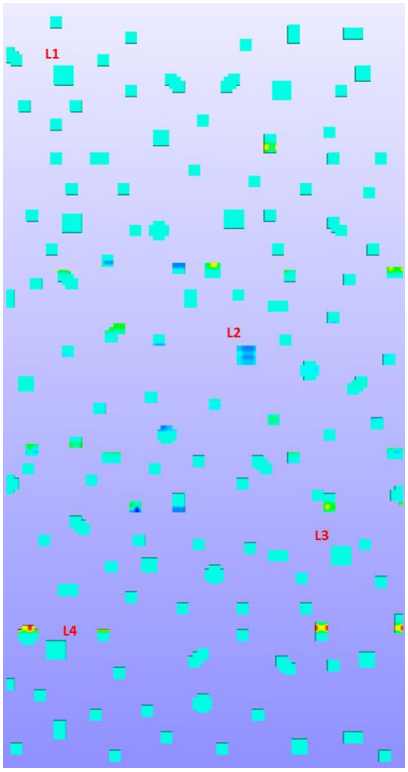

Figure 4-1: *Postview* of the Micro model with osteocytes to be analyzed (variation in position)

4.2.2 Variation based on Orientation:

Based on the fact that all osteocytes in the bone matrix are not oriented in the same way, our study considered the orientation as a contributor to the strain magnification phenomena. Hence, we considered four lacunae that were oriented differently with respect to the loading surface. In order to minimize the effect of position, we considered all the lacunae almost similarly distant from the loading surface. In figure 4-2, the lacunae were named as 1AD, 1BD, 2H and 2V of which 1 represents diagonally oriented and 2 represents aligned

upright. Notations A and B were used in order to distinguish between their orientations, D stands for Diagonal whereas H and V stands for Horizontal and Vertical respectively.

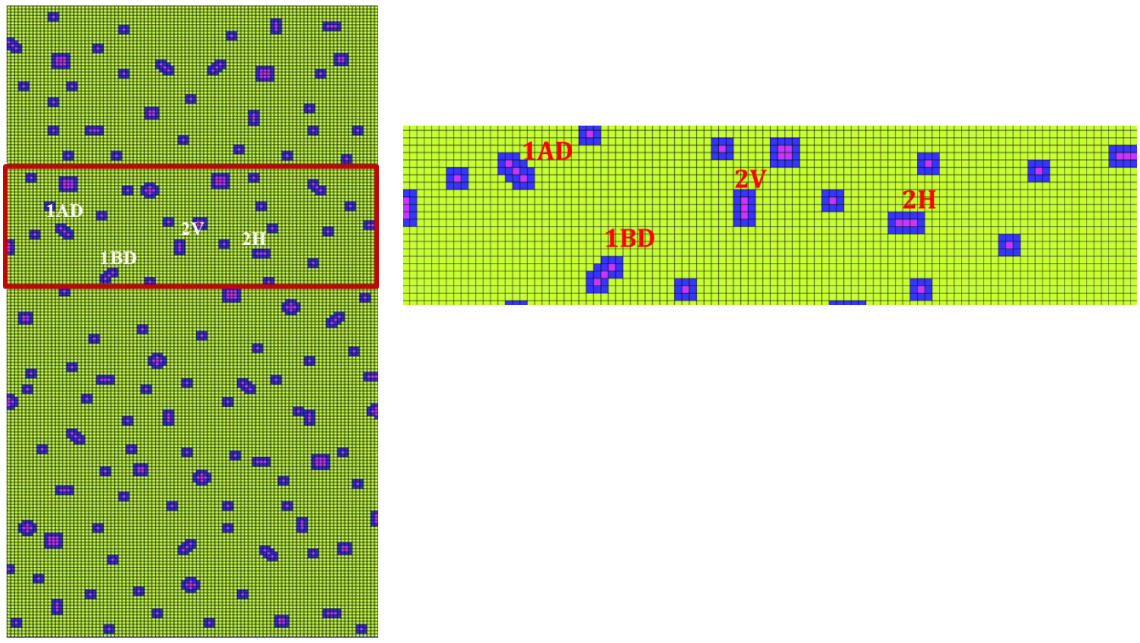

Figure 4-2: *Postview* of the Micro model with osteocytes to be analyzed (variation in orientation) and its magnified view (on the right)

4.2.3 Variation based on Size:

Through our literature survey, it had been found that all the osteocytes are not of the same size in the entire bone matrix. Understanding this fact, we have conducted a parametric study based on the variation in size of the osteocyte lacuna. In this study, we selected three lacunae of different sizes as shown in the figure 4-3. All the three selected lacunae were square shaped so as to remove the orientation effect. The notations for the lacunae represents its size: 1 for 1x1, 2 for 2x2 and 3 for 3x3 element size lacuna. As described in the above sections, size of each element was 10µmx10µm thereby making size of lacuna 1 as 10µmx10µm, lacuna 2 as 20µmx20µm and lacuna 3 as 30µmx30µm. In order to minimize the effect of position, I

had selected all the three lacunae close to each other.

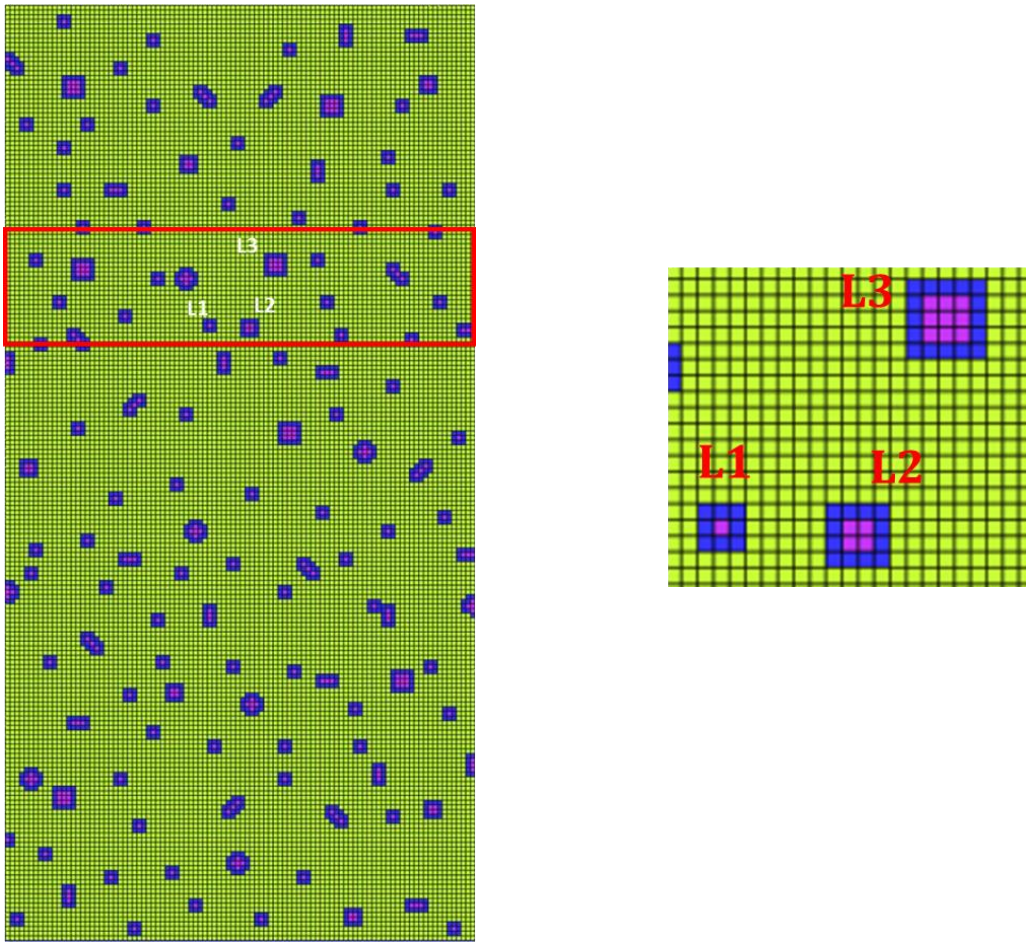

Figure 4-3: *Postview* of the Micro model with osteocytes to be analyzed (variation in size) and its magnified view (on the right)

4.3 Nano Model:

In the micro model created, the realistic size of the osteocyte as well as the density of the osteocytes in a human bone was considered parametrically. In order to extend the work to study the strains in the cell body, the fluid space in the lacuna and the perilacunar tissue, we created this model in the scale of nanometer as shown in the figure 4-4. The base for the size of the osteocyte was extracted from [13]Rochefort, *et al*., 2010 work on osteocytes which suggested a size of 10µm across the short axis and 20µm along the long axis of osteocyte. In

this study, due to the dimensional convenience, the size of each osteocyte was approximated to 20 µm x 8 µm x 4 µm and is fixed for all the osteocytes.

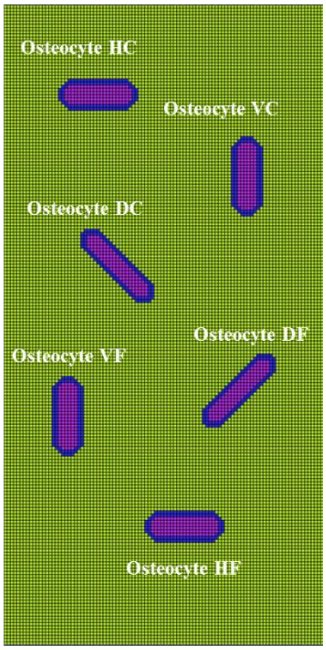

Figure 4-4: *Postview* of the Nano model with osteocytes to be analyzed

In this parametric study, as the size of the osteocyte is fixed, we focused on the positional variation along with the orientation variation effects on the lacunar lagrangian strains. Based on the studies on density of osteocytes, by scaling down the size of the bone matrix to 80 µm x 160 µm x 4 µm, we only had six osteocytes in our nanomodel. These six osteocytes were named according to their orientation as well as position as osteocyte HC, HF, osteocyte VC, VF and osteocyte DC, DF. Here, H, V, D stands for horizontal, vertical and diagonal respectively whereas C and F describes their positional difference as Close and Far with respect to the loading surface.

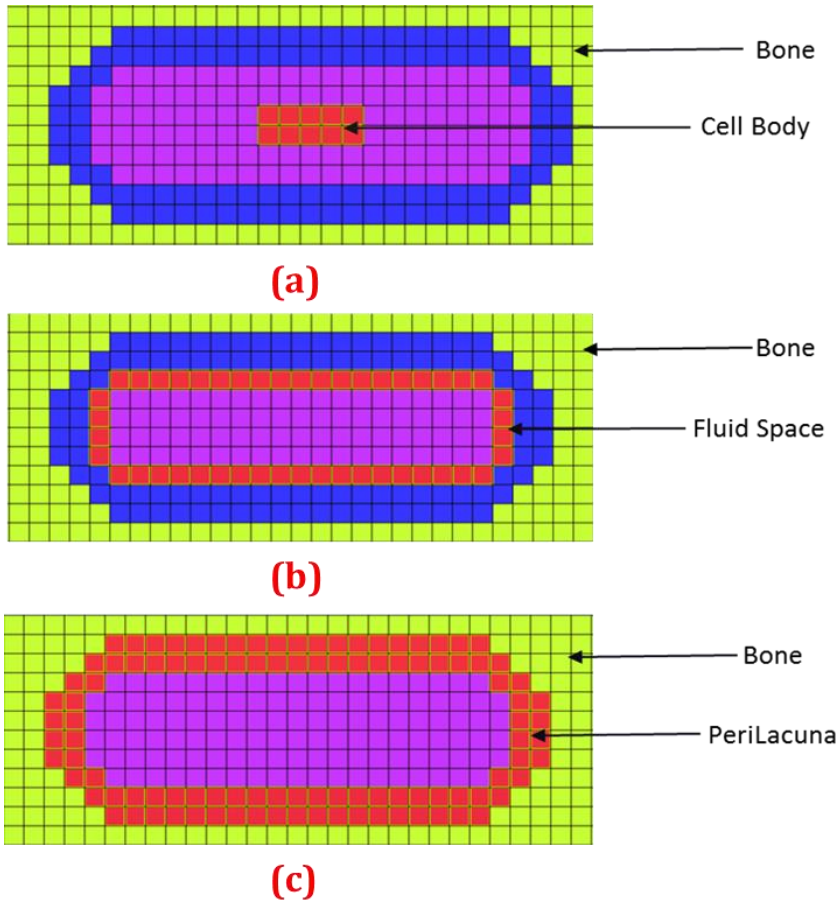

Figure 4-5: *Postview* sections of the Nano Model with partitions selected (in red color)

The analysis was done on the three respective portions of the osteocyte that were highlighted, in red, in each of the sub images in the figure 4-5 namely cell body, fluid space and the perilacuna.

4.4 Osteocyte 3D Model:

The osteocyte 3D model was created using MIMICS, 3-Matic softwares and was imported into *FEBio*. There were a total of 17 osteocytes (as shown in the figure 4-6) present in the entire model on which I had done a parametric study to obtain the strain response due to mechanical loading applied on one of the surfaces. All the osteocytes were oriented in the similar fashion and hence the study was based on the variation in size and position.

The osteocytes were classified as surface osteocytes and inner osteocytes. All the inner osteocytes were analyzed to observe the variation in size. The surface osteocytes were analyzed to study the variation in position.

Figure 4-6: *Postview* of Osteocyte 3D model with only osteocytes

CHAPTER 5

RESULTS AND DISCUSSIONS

5.1 Introduction:

This chapter deals with the results of our work and discussions based on the results. The results are organized in the same order as the models described earlier. First, the micro model was analyzed according to the parametric approach that was explained in the previous chapter i.e. by their position, orientation and size of the lacunae. All the results are tabulated and behavior of lacunae in response to the applied loading was studied. Similarly, the nano model was analyzed by considering the variation in position and orientation (as the size is same for all osteocytes). Then, the osteocyte 3D model was analyzed and the results obtained in this analysis are tabulated. In the later part of this chapter, we discuss the results by comparing each model with the previous models.

5.2 Micro Model:

The analysis was performed using the *Postview* software tool. The detailed explanation of measuring lagrangian strains are given in the Appendix-A. The parametric analysis was performed on the micro model by varying the perilacunar modulus and the results from the analysis are explained below. The observations and results are explained in the following sections according to the order in which they were analyzed.

5.2.1 Variation based on Position:

In this analysis, the four lacunae were named as L1, L2, L3 and L4 depending on their distance from the loading surface. Lacuna L1 is the nearest to the loading surface and L4 is the farthest. The strain magnification due to the positional variation was analyzed. The results from the analysis of micro model based on positional variation are tabulated in table

5-1. In table 5-1, the first column represents the variable of our parametric analysis 'Peri Lacunar Modulus' (Young's modulus of PeriLacunar tissue). Each osteocyte's lacunar strain responses are tabulated along with their ratio over bone strains.

Table 5-1: Comparison of Lacunar Strains and Strain magnification in Micro model - Variation in Position

Comparison of Lacunar Strains and Strain Magnification in Micro Model – Variation in Position								
	Lacuna L1		**Lacuna L2**		**Lacuna L3**		**Lacuna L4**	
Young's modulus (PeriLacunar Tissue)	Lacunar Strain	**L/B Ratio**	Lacunar Strain	**L/B Ratio**	Lacunar Strain	**L/B Ratio**	Lacunar Strain	**L/B Ratio**
5 GPa	9325	**4.66**	9167	**4.58**	9012	**4.51**	9000	**4.50**
10 GPa	8392	**4.20**	8168	**4.08**	7763	**3.88**	7713	**3.86**
15 GPa	7709	**3.85**	7390	**3.70**	6869	**3.43**	6798	**3.40**
20 GPa	7130	**3.57**	6760	**3.38**	6187	**3.09**	6102	**3.05**

From the table 5-1, the columns named L/B ratio represents the strain magnification ratio of lacunar strains to the bone strains of the respective osteocyte. In all the cases, the bone strain was fixed to 2000 με. The calculation of the bone strains was explained in section 3.6.

The strain ratio was decreased from 4.66 to 3.57 for osteocyte #L1 when the perilacunar modulus was increased from 5 GPa to 20 GPa. This shows that the strain values obtained for a lower perilacunar modulus were higher compared to that of lower strain values obtained for a higher perilacunar modulus. These results support [12]Bonivtch *et al*., 2006 work on strain amplification.

The magnification in strains due to mechanical loading was investigated in the Bonivtch's work by varying the perilacunar modulus. We have extended that work by varying the position of lacuna with respect to loading in addition to the perilacunar modulus variation.

For the perilacunar modulus of 5 GPa, the strain magnification ratio went down from 4.66 to 4.50 as the osteocyte distance from the loading surface increased. This suggests that the load experienced by the osteocyte nearer to the loading surface resulted in a larger strain when compared to the farther osteocyte.

5.2.2 Variation based on Orientation:

In this analysis, the four lacunae under analysis were named according to their orientation as lacuna #1AD, #1BD, #2V and #2H. Here, D, V and H stands for diagonal vertical and horizontal orientations respectively. A and B represents difference between two diagonal orientations.

The procedure that was explained in Appendix-A was applied in this model also in analyzing the model for estimating the strain magnification due to variation in orientation. Figure 5-1 represents the line graph between elastic modulus of peri lacuna on x-axis and maximum lacunar Y-lagrange strain on y-axis. The perilacunar modulus was varied from 5GPa to 20GPa and the lacunar strains in each osteocyte were measured and displayed on the graph. In the graph, the lacunar strains in each lacuna are represented using a line graph and the four lacunae under analysis are distinguished by using four different symbols for osteocytes #1AD, #1BD, #2V and #2H respectively as shown in figure 5-1.

Looking at the graph, it is evident that an increase in the elastic modulus of perilacuna from 5 GPa to 20 GPa results in a decrease in maximum lacunar strains in all the lacunae. For instance, the graph which represents osteocyte #2H, there was a decrease in lacunar strains from 17,027 με to 11,421 με with an increase in perilacunar modulus from 5 GPa to 20 GPa. A similar trend was observed in all the other lacunae.

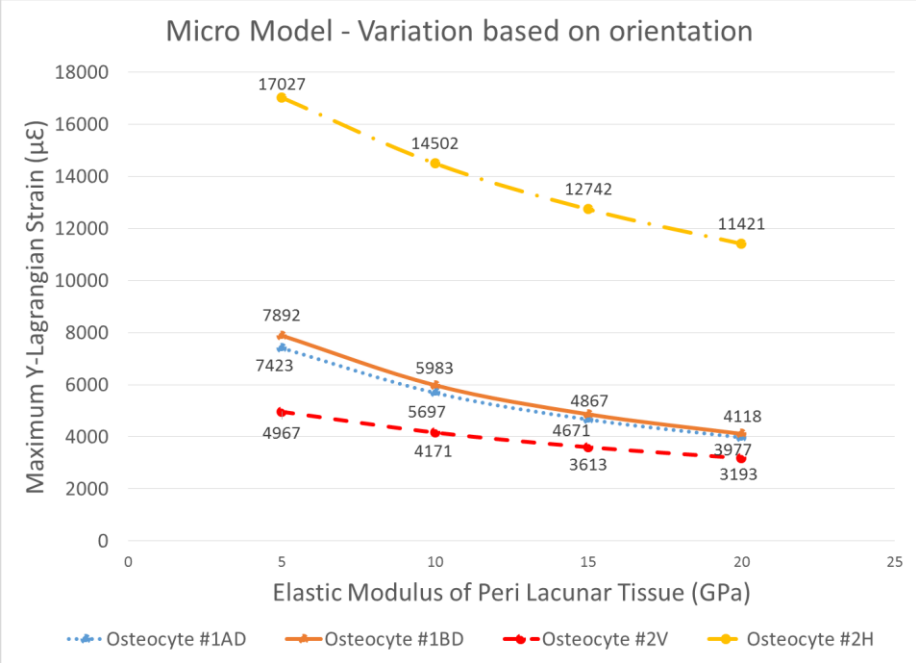

Figure 5-1: Comparison of lacunar strains based on variation in orientation

The lacuna #2H, which was oriented horizontal to the loading surface, experienced the highest strains when compared to all other lacunae whereas the lacuna #2V, which was oriented vertical to the loading surface experienced the lowest strains. In terms of numbers, for 5 GPa perilacunar modulus strains at lacuna #2H was 17,027 με vs 4,967 με at lacuna #2V. The lacunae that were oriented diagonally had almost a similar range of lacunar strains and the range was in between 17,027 με at #2H and 4,967 με at #2V.

5.2.3 Variation based on Size:

As explained in the parametric analysis section, the lacunar strains are analyzed in three lacunae of different sizes. Three lacunae that were analyzed in this model are labelled as lacuna #L1, #L2 and#L3 according to their sizes. Lacuna #L1 has only one element, #L2 has 2x2 elements and #L3 has 3x3 elements. The size of lacunae for these osteocytes were 10μmx10μm, 20μmx20μm and 30μmx30μm for lacunae #L1, #L2 and #L3 respectively.

The lacunar strain responses of the three lacunae are shown as a graphical representation in figure 5-2. These responses are represented as line graphs and three symbols are used in graph for distinguishing the lacunae as shown in figure 5-2.

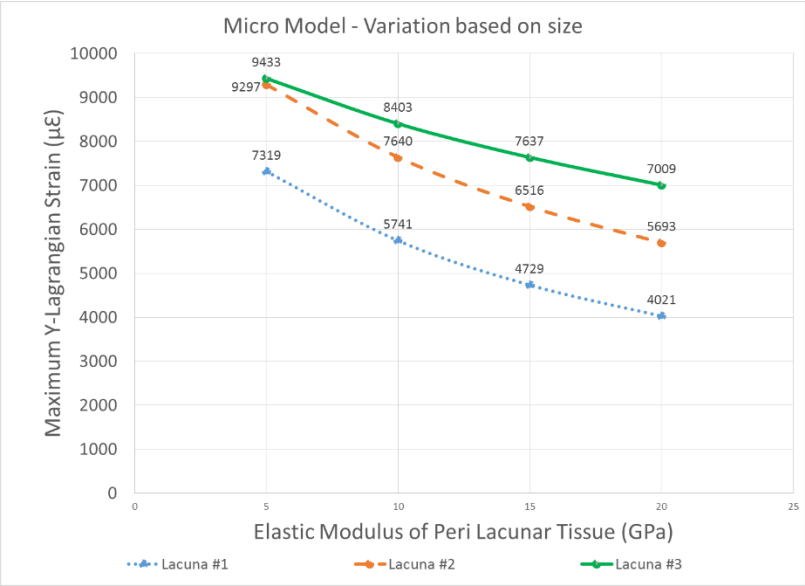

Figure 5-2: Comparison of lacunar strains based on variation in size

From the analysis results shown in figure 5-2, it is clear that the size of the lacunae had its impact on the lacunar strain response. At a particular perilacunar modulus (say 5 GPa), the lacunar strain values were 7,319 με, 9,297 με and 9,433 με for lacunae #L1, #L2 and #L3 respectively. This data suggests that an increase in size of the lacuna resulted in an increase in the lacunar strain value. In addition to this, lacunar strain decreased in all the lacunae with the increase in perilacunar modulus from 5 GPa to 20 GPa. For lacuna #L1, strain value decreased from 7,319 με at 5 GPa to 4,021 με at 20 GPa.

5.3 Nano Model:

Based on the results from the analysis on micro model, a nanomodel was designed using realistic size, density and shape of osteocytes that was scaled down to nano level. As discussed in section 3.3, this model had six osteocytes and were of the same size. These osteocytes were

named according to their orientation and position as osteocyte #HC, #HF, #DC, #DF, #VC and #VF where the first subscript represents orientation and the second subscript represents position. H, D and V represents horizontal, diagonal and vertical orientations respectively whereas C and F represents close and far respectively. The analysis was done using the same procedure given in Appendix-A.

The lacunar strain measurements were classified in to two categories namely cell body and fluid space lacunar strains. Each of them were analyzed separately and are tabulated in tables 5-2 and 5-3.

Table 5-2: Comparison of Fluid space Strains in Nano Model

Comparison of Microstrains in Fluid Space of the Osteocytes - Nano Model

	Osteocyte #HC		Osteocyte #HF		Osteocyte #VC		Osteocyte #VF		Osteocyte #DC		Osteocyte #DF	
Young's modulus (PeriLacunar Tissue)	Fluid space	L/B Ratio	Fluid space	L/B Ratio	Fluid space	L/B Ratio	Fluid space	L/B Ratio	Fluid space	L/B Ratio	Fluid space	L/B Ratio
5 GPa	17,482	**8.74**	15,526	**7.76**	4,194	**2.10**	3,995	**2.00**	11,418	**5.71**	12,213	**6.11**
10 GPa	16,276	**8.14**	14,616	**7.31**	3,901	**1.95**	3,722	**1.86**	10,501	**5.25**	11,185	**5.59**
15 GPa	15,372	**7.69**	13,926	**6.96**	3,668	**1.83**	3,502	**1.75**	9,821	**4.91**	10,430	**5.22**
20 GPa	14,654	**7.33**	13,371	**6.69**	3,472	**1.74**	3,316	**1.66**	9,286	**4.64**	9,841	**4.92**

From the table 5-2, the fluid space strains in all the osteocytes decreased as the perilacunar modulus increased from 5 GPa to 20 GPa. For osteocyte #HC, the fluid space strains were found to be decreased from 17,482 με for 5 GPa perilacunar modulus to 14,654

με for 20 GPa perilacunar modulus. The fluid space strain magnification was found highest in the osteocytes that were oriented horizontally and were least in the osteocytes that were oriented vertically i.e. for 5 GPa perilacunar modulus case, the strain magnification was found to be around ~9x for horizontally oriented osteocytes (HC & HF) compared against ~2x for vertical oriented ones (VC & VF) and ~6x for the diagonally oriented ones (DC & DF). These results appear to follow our previous studies on variation in orientation using the micro model.

There was a decrease in the fluid space strain value with the variation in position from 17,482 με for osteocyte #HC to 15,526 με for osteocyte #HF at 5 GPa perilacunar modulus. whereas it was less than 5% decrease for osteocytes #VC to #VF. With these results, it is evident that not only orientation had its effect on the fluid space lacunar strains but also the variation in position has its impact.

Table 5-3: Comparison of Cell Body Lacunar Strains in Nano Model

Comparison of Microstrains in Cell Body of the Osteocytes - Nano Model

	Osteocyte #HC		Osteocyte #HF		Osteocyte #VC		Osteocyte #VF		Osteocyte #DC		Osteocyte #DF	
Young's modulus (PeriLacunar Tissue)	Fluid space	L/B Ratio	Fluid space	L/B Ratio	Fluid space	L/B Ratio	Fluid space	L/B Ratio	Fluid space	L/B Ratio	Fluid space	L/B Ratio
5 GPa	20690	**10.34**	18354	**9.18**	3802	**1.90**	3456	**1.73**	17946	**8.97**	19482	**9.74**
10 GPa	19686	**9.84**	17671	**8.84**	3558	**1.78**	3252	**1.63**	16924	**8.46**	18206	**9.10**
15 GPa	18839	**9.42**	17062	**8.53**	3347	**1.67**	3070	**1.53**	16075	**8.04**	17234	**8.62**
20 GPa	18159	**9.08**	16566	**8.28**	3160	**1.58**	2905	**1.45**	15387	**7.69**	16456	**8.23**

Table 5-3 shows the data of cell body strains and their ratios with respect to bone strains (strain magnification ratio) measured at different perilacunar modulus values. There was a decrease in cell body strains in all the osteocytes as the perilacunar modulus increased from 5 GPa to 20 GPa. For osteocyte #HC, the cell body strains decreased from 20,690 με for 5 GPa perilacunar modulus to 18,159 με for 20 GPa perilacunar modulus. There was an increase in cell body strains compared to that of fluid space strains for horizontally oriented (HC & HF) and diagonally oriented (DC & DF) osteocytes. At 5 GPa perilacunar modulus, there was an increase in strains from 17,482 με at fluid space to 20,690 με at cell body for osteocyte #HC and there was an increase in strains from 11,418 με at fluid space to 17,946 με at cell body for osteocyte #DC whereas the strains were decreased from 4,194 με at fluid space to 3,802 at cell body for osteocyte #VC. As only ten elements at the center of the lacunae were used for computing the cell body strain, there was a possibility of having the impact of surrounding lacunae on these ten elements. This was the reason for an increase in the cell body strains when compared with the fluid space strains.

From table 5-3, it is clear that an increase in the perilacunar modulus resulted in a decrease in the cell body strains irrespective of their position or orientation. In addition, the observations on variation in position mentioned in the fluid space strain case were also seen here i.e farther the osteocyte from loading surface, lesser was the cell body strain. At 5 GPa perilacunar modulus, osteocyte #HC has 20,690 με cell body strains whereas while osteocyte moved farther from loading surface it is decreased to 18,354 με for osteocyte #HF.

5.4 Osteocyte 3D Model:

The Osteocyte 3 D model was designed by using confocal images from a 5-month old female mouse femur. As all the osteocytes were oriented in a similar fashion, the analysis of

Osteocyte 3D model was designed in such a way that the variation in size and variation in position were observed.

In the analysis of osteocyte 3D model, all the 17 osteocytes were classified based on their position as inner osteocytes or surface osteocytes. Only inner osteocytes were considered in the comparison based on the size of the osteocytes. As it is difficult to calculate the number of elements that are on the surface. The inner osteocytes strain responses were tabulated in table 5-4 in the increasing order of their sizes.

Table 5-4: Comparison of Lacunar Strains in Osteocyte 3 D Model – Variation in Size

Comparison of Microstrains Based on the Size of Osteocytes (Inner Osteocytes) – Osteocyte 3D Model			
Osteocyte	# of elements	Max (μƐ)	Lacuna/Bone Ratio
O3	278	3481	**1.74**
O2	310	4042	**2.02**
O9	354	4266	**2.13**
O7	389	4124	**2.06**
O14	425	3976	**1.99**
O11	425	4221	**2.11**
O12	447	5681	**2.84**
O6	467	5319	**2.66**
O5	705	5821	**2.91**

From the table 5-4, the osteocytes that were inside the bone matrix i.e. inner osteocytes were having the lacunar to bone ratio in the range of 1.74 to 2.91 in which 1.74 was the ratio of osteocyte O3 which was the smallest sized osteocyte among these inner osteocytes and 2.91 was the ratio of largest sized osteocyte among inner osteocytes i.e. O5. This means that the

lacunar strain magnification was affected by the size of the osteocyte. Not only size of the osteocyte, positional variation has also impacted the lacunar strains in the osteocytes like O11 and O14 which are having the 425 elements but the difference in their position made the difference in strain magnification ratio i.e. 2.11 for O11 and 1.99 for O14.

The surface osteocytes were again sub-classified as top, side or bottom surface osteocytes. The lacunar strains in the surface osteocytes measured at each osteocyte location were tabulated in the table 5-5. In this analysis, the positional variation alone is considered because the number of elements on the surface may limit considering size of osteocytes.

Table 5-5: Comparison of Lacunar Strains in Osteocyte 3 D Model (Surface Osteocytes) – Variation in Position

Comparison of Microstrains Based on the Position of Osteocytes (Surface Osteocytes) – Osteocyte 3D Model				
Surface	Lacuna	# of elements	Max (με)	Lacuna/Bone Ratio
TOP	O16	876	7093	**3.55**
	O4	1066	12472	**6.24**
	O17	1415	4180	**2.09**
SIDE	O1	361	6052	**3.03**
	O15	458	4691	**2.35**
BOTTOM	O10	351	4071	**2.04**
	O13	559	2986	**1.49**
	O8	566	5268	**2.63**

The lacuna to bone strain ratio in the bottom surface lacunae were lower when compared with the top and side surfaces which depicts that the positional variation is also having a major impact on the magnification of lacunar strains. The osteocytes that were on the top surface or loading surface were having highest lacuna to bone strain ratios i.e 6.24.

The osteocytes that were on the side surface experience a strain magnification of around ~3x and the osteocytes that were on the bottom surface experience a strain magnification of around 2x. Osteocyte O1 which has only 361 elements has a magnification ratio of 3.03 compared to 1.49 of O13 which has 559 elements because some part of O1 was on the side surface whereas O13 was on bottom surface.

Osteocyte O17 which has highest number of elements and also is on the top surface has a strain magnification ratio of 2.09. This may be because of the number of elements that were on the surface and the shape of the osteocyte may have had an impact. These kind of cases are of our future interest which can be evaluated by calculating number of elements on the surface.

CHAPTER 6

DISCUSSIONS

This chapter discusses on all the work we have done and their results in reference to each model in the order they were created. This gives a brief summary of our results and the interpretations from the results. At the end of this chapter, limitations in this work are discussed.

6.1 Micro Model:

Variation in Position:

The impact of positional variation on strain magnification was studied by varying the distance of lacunae from the loading surface. As the lacunae distance from loading increases, the lacunar strain and thereby strain magnification ratio decreases. In addition to these results, we have also found that the perilacunar modulus had its impact on the strain magnification ratio. As the perilacunar modulus increases from 5 GPa to 20 GPa, the strain magnification ratio decreases.

Variation in Orientation:

In this analysis, we have considered the lacunae of different orientation but are of same size and are positioned almost at the similar distance from the loading surface so as to remove the size and position effect on the strain magnification. The lacunae that were oriented horizontally has the highest strain magnification ratio and the vertical lacunae have the least strain magnification ratio. The lacunae with diagonal orientation have the ratio's in between vertical and horizontal lacunae. Similar to the previous study, as the perilacunar modulus increases from 5 GPa to 20 GPa, the strain magnification ratio decreases.

Variation in Size:

In order to observe the strain magnification due to variation in size, three lacunae of different sizes were considered in this analysis. All the lacunae were square shaped and were almost at the same distance from the loading surface so as to remove the orientation and positional effect. As the size of the lacunae was increased, the lacunar strain value increased. It was concluded that all the three parameters, position, orientation and size, have their impact on the magnification of strain in the lacuna. Similar to the previous studies, as the perilacunar modulus increases from 5 GPa to 20 GPa, the strain magnification ratio decreases.

6.2 Nano Model:

By considering all the parameters from the micro model that effect strain magnification, we have created this model with six osteocytes. The size of each osteocyte was taken as 20µmx8µmx4µm. In this analysis, the orientation and position effects on strain magnification were considered. The strain magnifications were analyzed at two lacunar locations namely fluid space and cell body. The strain magnification found in cell body were higher compared to that of fluid space for the osteocytes oriented horizontally and diagonally. In case of vertical osteocytes, strains found in fluid space are higher than cell body.

In both fluid space and cell body, strain magnification ratio was found highest for horizontally oriented osteocytes and least for vertically oriented osteocytes. Diagonally oriented osteocytes have the ratios in between horizontal and vertical ones. These results support our micro model results for variation in orientation.

The strain magnification ratio decreased for the osteocytes of same orientation but are positioned farther from the loading surface. These results support our micro model for variation in position.

The perilacunar modulus effect can also be seen in this model. Our results support [12]Bonivtch's, 2006 work on strain amplification which concluded that an increase in perilacunar modulus results in a decrease in strain magnification.

6.3 Osteocyte 3D Model:

A more realistic model created using confocal image stacks of 5-month old mouse femur was analyzed based on the previous analysis procedures used. The osteocytes were classified as inner and surface osteocytes. Inner osteocytes were analyzed to see the variation in size and from these results it was observed that the increase in size lead to the increase in strain magnification. Surface osteocytes were considered for analyzing the model based on the variation in position. From these results, it is evident that the osteocytes that are on the top surface (loading surface) are experiencing more strain magnification compared to that of the osteocytes that were on the bottom surface.

6.4 Limitations of our work:

- Although we know that bone is anisotropic in nature, in this thesis work, we have created the models considering that the bone is isotropic.
- Size of the osteocyte is not a fixed value, but in order to minimize the modeling complexity we have considered the size of the osteocyte to be constant in the nano model.
- Shape of the osteocyte is not a perfect ellipsoid, in fact it is irregular in shape, but we have designed it to be a perfect ellipsoid to avoid dimensional complexities.

CHAPTER 7

CONCLUSION AND FUTURE WORK

The finite element model created using *FEBio* software suite helped us to measure the strain amplification responses in the osteocyte lacuna due to the mechanical loading applied. The effect of parameters like position, orientation and size on the lacunar strain amplification were observed. The parametric analysis performed on the model by increasing the perilacunar modulus resulted in a decrease of lacunar strain. Finally, we had designed a more realistic osteocyte 3D model which was developed by importing osteocyte images from the mouse femurs into *FEBio* and measuring the strain responses due to loading. The impact of position and size variations on lacunar stain amplification were measured.

The lacunar strain magnification ratio decreased as the distance of lacunae increased from the loading surface. Thus the impact of loading on lacunae is less at a farther distance from the loading surface. The strain magnification ratio decreases in the order of horizontal to diagonal to vertical orientation which means that horizontally oriented lacunae experience more strain magnification compared to that of other lacunae. As the size of the osteocyte increases, the strain magnification ratio increases. The combined effect of position and size is discussed in the osteocyte 3D model and has to be studied further by calculating the exact position of osteocyte in the 3-dimensional space.

The future scope of our work is…

(i) To measure the exact position of the osteocyte and its distance from the loading surface in the osteocyte 3D model.

(ii) To study the impact of the presence of canaliculi on lacunar strains by modeling our existing models with canaliculi.

(iii) Design osteocyte 3D model by incorporating the osteocytes that were oriented differently in order to see the impact of variation in orientation on lacunar strains.

APPENDIX - A

STEP-BY-STEP PROCEDURE IN THE ANALYSIS

Step #1: Open *Postview* file.

Double click on the *Postview* (.xplt) file. If the default opening type is not *Postview*, then navigate to the *Postview* folder and make it as default type for opening these type of files.

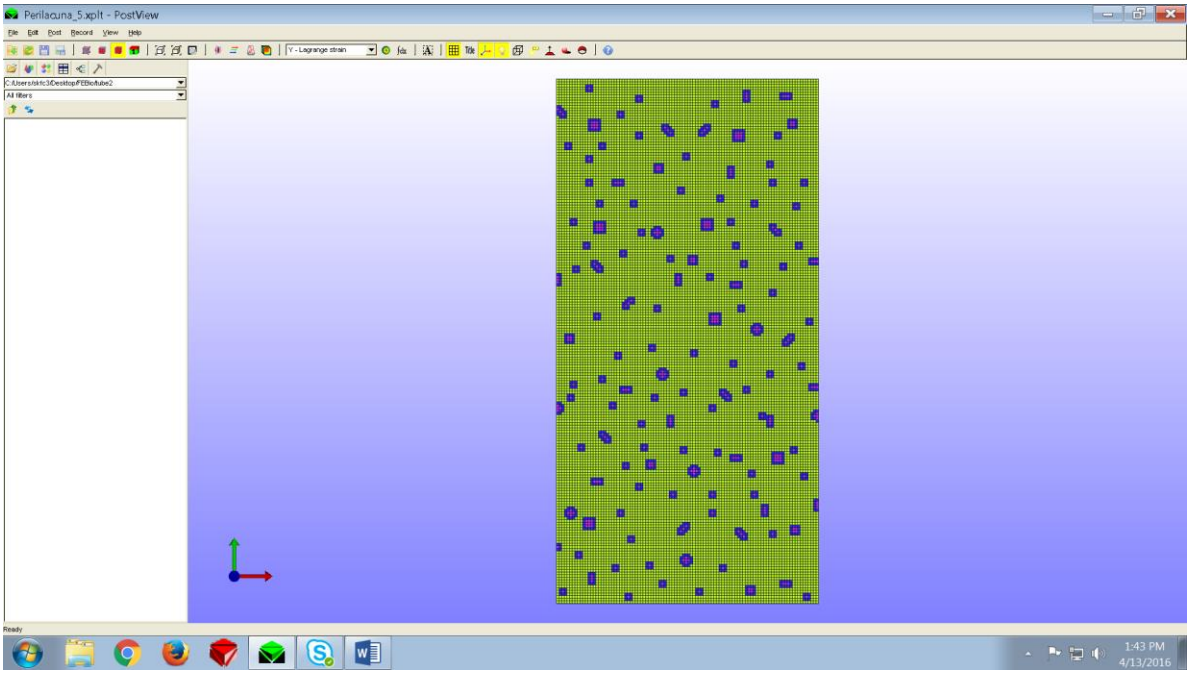

Figure A-1: *Postview* user interface

Step #2: Selection of the y-variable for analysis.

After opening the .xplt file, the finite element model will appear in the *Postview* user interface as shown in the above figure. In this interface, we can select a y-variable from a drop down list. The list of y-variables include displacement, position, stress, lagrangian strain and pressure and variations on each of these can be viewed in all the three dimensions. In our model, as the loading has been applied in the Y-direction, we have focused on calculating the Y- lagrange strain. This selection of variable can be seen in the figure below.

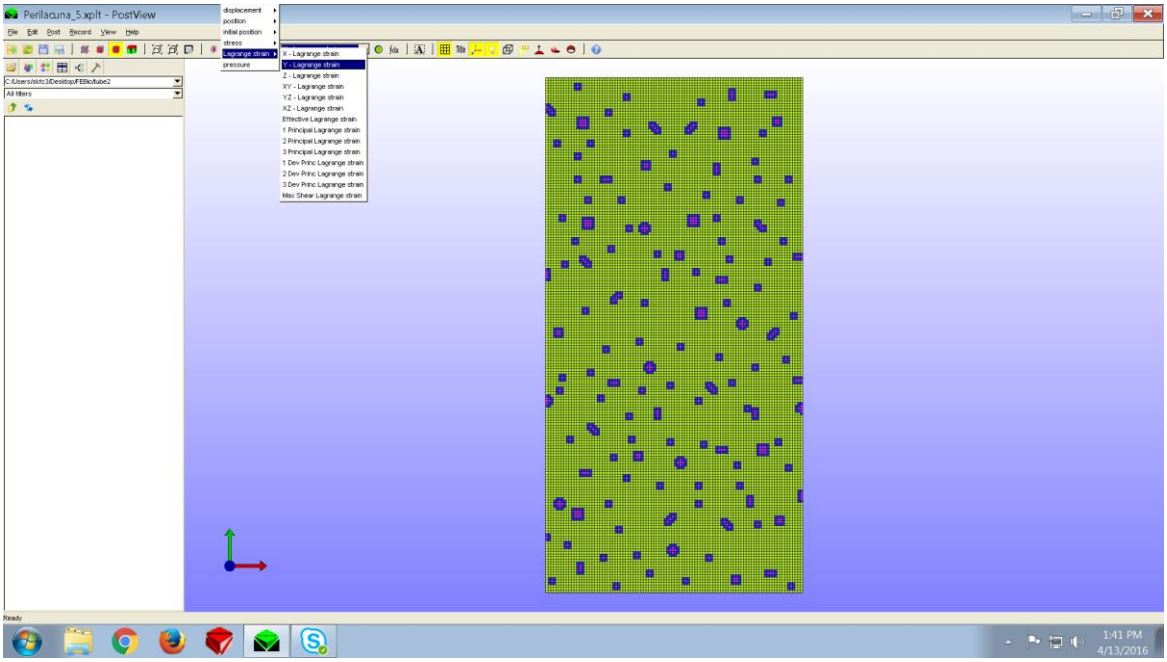

Figure A-2: Selection of y-variable for analysis

Step #3: Hiding the bone material.

By clicking on the materials manager tool bar icon, we can select one of the three materials that were used in this model and can be hidden. So that, we can only see the partition of the osteocyte that was being analyzed. In figure A-3, the bone material was hidden and only lacuna and perilacuna were focused as our analysis was concentrated on calculating the launar and perilacunar strains.

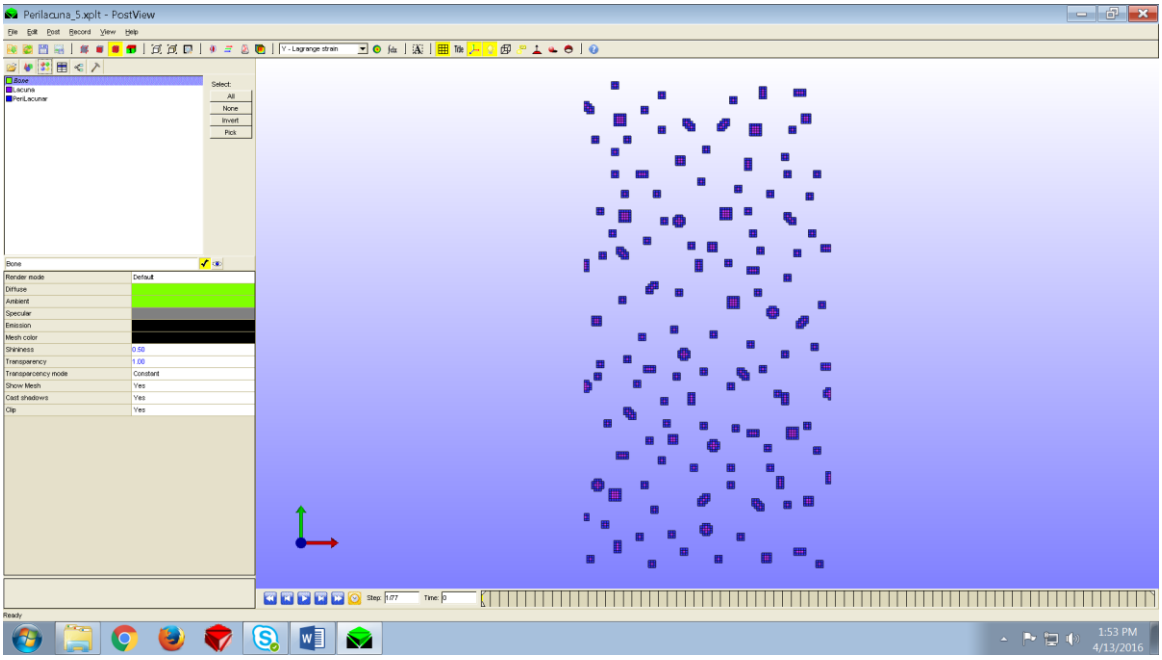

Figure A-3: Hiding bone material by using materials manager

Step #4: Trackview of the element (or group of elements).

In the finite element model, to analyze an element or a group of elements, we need to zoom-in to the respective element on which analysis was to be performed. We can zoom-in or zoom-out the model in *Postview* interface by holding the right button on mouse and dragging the mouse forward or backward respectively. In this step, we select an element or a group of elements and their lagrangian strains with respect to the time instants were displayed by using the Trackview option in the drop down list of 'Post' menu bar item or simply by pressing F3. Then, a graph will be displayed with Y-lagrange strain as y-variable and time steps as x-variable as shown in figure A-4. In the Trackview window, an option to save these results is available at the top left corner. By click this icon, the lagrangian strain values that were measure with respect to time instants will be saved as a text file.

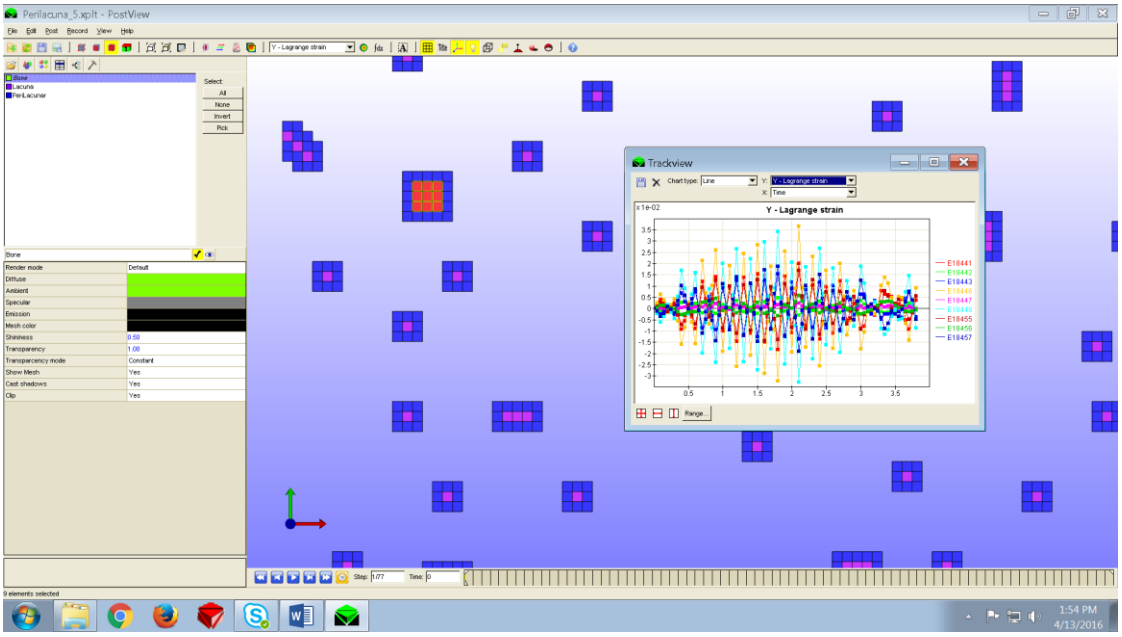

Figure A-4: Trackview of the selected elements

Step #5: Importing text file into excel.

The text file created in the above step will now be imported into excel by using the import option in the excel sheet. In the figure below, the first column is time and the next 9 columns represents the 9 elements under analysis. The average of all the nine elements was calculated at each time instant and were tabulated in the column named S1_Avg. The strain values were scaled to microstrain (με) values by multiplying with a factor of 10^6. These were the values used in the analysis and comparison with other osteocytes.

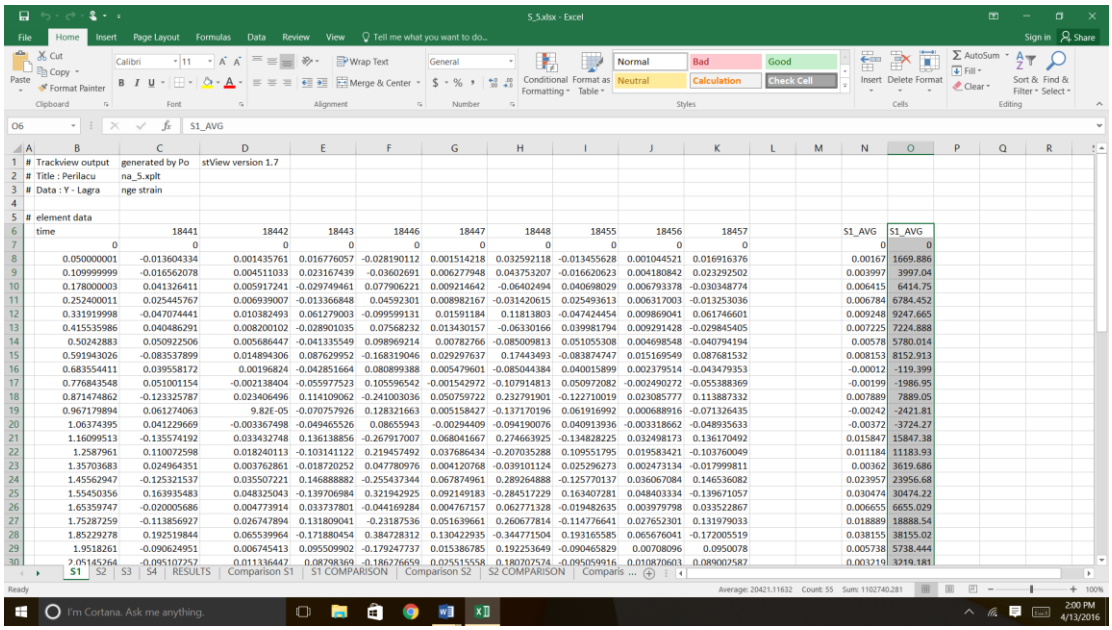

Figure A-5: Importing the text file into excel and calculating average strain

Step #6: Comparing the results.

The above procedure was applied to all other osteocytes for calculating the strain values and were tabulated.

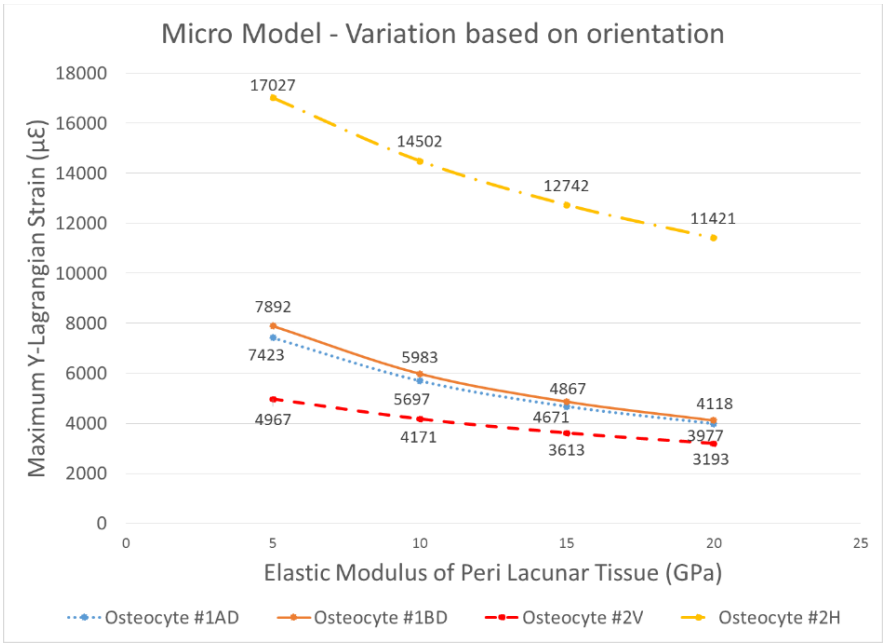

Figure A-6: Graphical representation of the obtained results

The above procedure was applied for the remaining perilacunar modulus values in our parametric study. These values were compared with each other and were presented in the graphical form as shown in figure A-6. This was the procedure used to analyze all the models.

BIBLIOGRAPHY

1. Buenzli, P.R. and N.A. Sims, *Quantifying the osteocyte network in the human skeleton.* Bone, 2015. **75**: p. 144-150.
2. Orr, A.W., et al., *Mechanisms of Mechanotransduction.* Developmental Cell, 2006. **10**(1): p. 11-20.
3. Santos, A., A.D. Bakker, and J. Klein-Nulend, *The role of osteocytes in bone mechanotransduction.* Osteoporosis International, 2009. **20**(6): p. 1027-1031.
4. Huang, C. and R. Ogawa, *Mechanotransduction in bone repair and regeneration.* The FASEB Journal, 2010. **24**(10): p. 3625-3632.
5. Forwood, M.R., et al., *Increased bone formation in rat tibiae after a single short period of dynamic loading in vivo.* Am J Physiol Endocrinol Metab, 1996. **270**(3): p. E419-423.
6. Lanyon, L.E., *Osteocytes, strain detection, bone modeling and remodeling.* Calcified Tissue International, 1993. **53**(0): p. S102-S107.
7. Robling, A. and C. Turner, *Mechanotransduction in bone: genetic effects on mechanosensitivity in mice.* Bone, 2002. **31**(5): p. 562-569.
8. Burr, D., A. Robling, and C. Turner, *Effects of biomechanical stress on bones in animals.* Bone, 2002. **30**(5): p. 781-786.
9. Kim, D., J. Brunski, and D. Nicolella, *Microstrain fields for cortical bone in uniaxial tension: optical analysis method.* Proceedings of the Institution of Mechanical Engineers, Part H: Journal of Engineering in Medicine, 2005. **219**(2): p. 119-128.
10. Rath Bonivtch, A., L.F. Bonewald, and D.P. Nicolella, *Tissue strain amplification at the osteocyte lacuna: A microstructural finite element analysis.* Journal of Biomechanics, 2007. **40**(10): p. 2199-2206.
11. Maas, S.A., et al., *FEBio: finite elements for biomechanics.* Journal of biomechanical engineering, 2012. **134**(1): p. 011005.
12. Bonivtch, A.R., L.F. Bonewald, and D.P. Nicolella, *Tissue strain amplification at the osteocyte lacuna: a microstructural finite element analysis.* Journal of biomechanics, 2007. **40**(10): p. 2199-2206.
13. Rochefort, G.Y., S. Pallu, and C.L. Benhamou, *Osteocyte: the unrecognized side of bone tissue.* Osteoporosis international, 2010. **21**(9): p. 1457-1469.

VITA

Sravan Kumar Reddy Kola was born in Hyderabad, in the state of Andhra Pradesh, India on July 1st, 1991. He graduated with his Bachelor's degree in Electronics and Communications Engineering from Jawaharlal Technological University, Kakinada in 2013. With a lot enthusiasm and zeal to pursue higher education, he opted and enrolled at University of Missouri-Kansas City for doing his Masters in Electrical Engineering during fall 2014. As soon as he started his masters, his previous experience in India brought him an opportunity to work as a Graduate Research Assistant under Dr. Ganesh Thiagarajan. The research thesis focuses on developing finite element models to study the lacunar strain responses in an osteocyte. He is currently working as a Software Test Engineer at GHSP – Solutions in Motion, Grand Haven, MI.

Email ID: skfc3@mail.umkc.edu

This thesis was typed by the author.